
Report No. FHWA-KS-07-1

FINAL REPORT

**EVALUATING THE TIME-DEPENDENT
DEFORMATIONS AND BOND CHARACTERISTICS
OF A SELF CONSOLIDATING CONCRETE MIX
AND THE IMPLICATION FOR PRETENSIONED
BRIDGE APPLICATIONS**

Kyle H. Larson, Ph.D.
Robert J. Peterman, Ph.D., P.E.
Asad Esmaeily, Ph.D.
Kansas State University

April 2007

KANSAS DEPARTMENT OF TRANSPORTATION

**Division of Operations
Bureau of Materials and Research**



1 Report No. FHWA-KS-07-1	2 Government Accession No.	3 Recipient Catalog No.	
4 Title and Subtitle EVALUATING THE TIME-DEPENDENT DEFORMATION AND BOND CHARACTERISTICS OF A SELF-CONSOLIDATING CONCRETE MIX AND THE IMPLICATIONS FOR PRETENSIONED BRIDGE APPLICATIONS		5 Report Date April 2007	6 Performing Organization Code
		8 Performing Organization Report No.	
7 Author(s) Kyle H. Larson, Ph.D., Robert J. Peterman, Ph.D., P.E., Asad Esmaily, Ph.D.		10 Work Unit No. (TRAIS)	
9 Performing Organization Name and Address Kansas State University 215 Durland Manhattan, KS 66506		11 Contract or Grant No. C1440	
		13 Type of Report and Period Covered Final Report October 2002 - December 2006	
12 Sponsoring Agency Name and Address Kansas Department of Transportation Bureau of Materials and Research 700 SW Harrison Street Topeka, Kansas 66603-3754		14 Sponsoring Agency Code RE-0359-01	
		15 Supplementary Notes For more information write to address in block 9.	
16 Abstract <p>Results of an extensive experimental program conducted to determine the material, bond characteristics, and time-dependent deformations of a proposed self-consolidating concrete (SCC) mixture for bridge girders are presented. This research program was completed in three phases. The first phase consisted of 15 full-scale, pretensioned SCC flexural specimens tested to evaluate their transfer and development lengths. These specimens included both single-strand and multiple-strand beams, as well as specimens designed to evaluate the so-called "top-strand" effect. The top-strand specimens, with more than 20 inches of concrete below the strand, were tested to evaluate the current American Association of State Highway Officials requirement of a 30% increase in the development length when the concrete below the strand is more than 12 inches. Strand end-slip measurements, used to estimate transfer lengths, indicated the proposed SCC mixture meets ACI and AASHTO requirements. In addition, flexural tests confirmed the proposed SCC mixture also meets current code requirements for development length.</p> <p>The second phase was to evaluate the elastic shortening, creep, and shrinkage properties of the proposed SCC mixture for bridge girders. Four bridge girders with an inverted-T profile were used to measure these time-dependent deformations. In two of the specimens, the strands were tensioned to 75% of the ultimate tensile strength, simulating a girder at service. Strands of the other two specimens were left untensioned to evaluate shrinkage effect of the concrete alone. The shrinkage was then subtracted from the fully tensioned specimens and elastic shortening and creep were isolated after relaxation losses were calculated from code expressions. In addition, the fully tensioned specimens were used to determine transfer lengths of the prestressing strand.</p> <p>The final phase of the program was to record strain measurements of the actual bridge girders used in the field. Elastic shortening, creep, and shrinkage prestress losses of the proposed SCC mixture were compared with current design equations. Instrumentation of seven pretensioned girders in a five-span bridge located in Cowley County, Kansas, was used to measure time-dependent deformations. Three of these girders utilized SCC, while the other four were cast with conventional concrete.</p>			
17 Key Words Bridge Deck, Fiber Reinforced Polymer, FRP, Girder, Steel and Strain Gauge		18 Distribution Statement No restrictions. This document is available to the public through the National Technical Information Service, Springfield, Virginia 22161	
19 Security Classification (of this report) Unclassified	20 Security Classification (of this page) Unclassified	21 No. of pages 252	22 Price

**EVALUATING THE TIME-DEPENDENT
DEFORMATIONS AND BOND CHARACTERISTICS
OF A SELF CONSOLIDATING CONCRETE MIX
AND THE IMPLICATION FOR PRETENSIONED
BRIDGE APPLICATIONS**

Final Report

Prepared by

Kyle H. Larson, Ph.D.

Robert J. Peterman, Ph.D., P.E.

Asad Esmaeily, Ph.D.

A Report on Research Sponsored By

THE KANSAS DEPARTMENT OF TRANSPORTATION
TOPEKA, KANSAS

and

KANSAS STATE UNIVERSITY

April 2007

© Copyright 2007, **Kansas Department of Transportation**

NOTICE

The authors and the state of Kansas do not endorse products or manufacturers. Trade and manufacturers names appear herein solely because they are considered essential to the object of this report.

This information is available in alternative accessible formats. To obtain an alternative format, contact the Office of Transportation Information, Kansas Department of Transportation, 700 SW Harrison Street, Topeka, Kansas 66603-3754 or phone (785) 296-3585 (Voice) (TDD).

DISCLAIMER

The contents of this report reflect the views of the authors who are responsible for the facts and accuracy of the data presented herein. The contents do not necessarily reflect the views or the policies of the state of Kansas. This report does not constitute a standard, specification or regulation.

Abstract

Results of an extensive experimental program conducted to determine the material, bond characteristics, and time-dependent deformations of a proposed self-consolidating concrete (SCC) mixture for bridge girders are presented. This research program was completed in three phases. The first phase consisted of 15 full-scale, pretensioned SCC flexural specimens tested to evaluate their transfer and development lengths. These specimens included both single-strand and multiple-strand beams, as well as specimens designed to evaluate the so-called "top-strand" effect. The top-strand specimens, with more than 20 inches of concrete below the strand, were tested to evaluate the current American Association of State Highway Officials requirement of a 30% increase in the development length when the concrete below the strand is more than 12 inches. Strand end-slip measurements, used to estimate transfer lengths, indicated the proposed SCC mixture meets ACI and AASHTO requirements. In addition, flexural tests confirmed the proposed SCC mixture also meets current code requirements for development length.

The second phase was to evaluate the elastic shortening, creep, and shrinkage properties of the proposed SCC mixture for bridge girders. Four bridge girders with an inverted-T profile were used to measure these time-dependent deformations. In two of the specimens, the strands were tensioned to 75% of the ultimate tensile strength, simulating a girder at service. Strands of the other two specimens were left untensioned to evaluate shrinkage effect of the concrete alone. The shrinkage was then subtracted from the fully tensioned

specimens and elastic shortening and creep were isolated after relaxation losses were calculated from code expressions. In addition, the fully tensioned specimens were used to determine transfer lengths of the prestressing strand.

The final phase of the program was to record strain measurements of the actual bridge girders used in the field. Elastic shortening, creep, and shrinkage prestress losses of the proposed SCC mixture were compared with current design equations. Instrumentation of seven pretensioned girders in a five-span bridge located in Cowley County, Kansas, was used to measure time-dependent deformations. Three of these girders utilized SCC, while the other four were cast with conventional concrete.

ACKNOWLEDGMENTS

The authors would like to thank the Federal Highway Administration (FHWA) and the Kansas Department of Transportation (KDOT) for funding this project. The authors would also like to acknowledge the following personal for their contributions that enabled the successful completion of project.

Thanks are extended to David Meggers, KDOT Bureau of Materials and Research, whose help with all phases of the research project was greatly appreciated. Appreciation is also extended to Tom Bergquist and other personnel at Prestressed Concrete Inc, of Newton Kansas for their help with coordination and fabrication of specimens and girders for this project. Thanks are also given to personnel at Bridges, Inc of Newton Kansas for assistance during all phases of bridge construction.

Finally, the authors would like to thank Ken Hurst and Loren Risch of the KDOT State Bridge Office and Steve Toillion of FHWA for the interest and continuous support and feedback.

TABLE OF CONTENTS

ABSTRACT	II
ACKNOWLEDGMENTS	IV
LIST OF FIGURES	VIII
LIST OF TABLES.....	X
CHAPTER ONE - INTRODUCTION	1
1.1 BACKGROUND	2
1.2 TEST PROGRAM.....	6
1.2.1 OVERVIEW OF EXPERIMENTAL PROGRAM	6
1.2.1.1 TRANSFER LENGTH	6
1.2.1.1 DEVELOPMENT LENGTH.....	6
1.2.2 INVERTED-T-SHAPE SPECIMENS.....	7
1.2.3 COWLEY COUNTY BRIDGE.....	7
1.3 SCOPE.....	7
CHAPTER TWO - BACKGROUND & LITERATURE REVIEW	9
2.1 PRESTRESSED CONCRETE	9
2.1.1 CONCEPTS	9
2.1.2 DEFINITIONS.....	10
2.1.3 PRESTRESS LOSS EQUATIONS.....	11
2.2 SELF-CONSOLIDATING CONCRETE.....	12
2.3 ELEMENTS OF BOND.....	13
2.4 Current Development and Transfer Length Equations.....	30
2.5 Bridge Monitoring	30
CHAPTER THREE - DESIGN OF FLEXURAL SPECIMENS.....	33

3.1 Single-Strand Development Length Specimens.....	33
3.2 Multiple-Strand Development Length Specimens	37
3.3 Embedment Lengths.....	39
CHAPTER FOUR - MATERIAL PROPERTIES	45
4.1 Large-Block Pullout Tests	45
4.2 Mix Design	46
4.3 Fresh Concrete Evaluation	47
4.4 Hardened Concrete Properties.....	50
CHAPTER FIVE - DETERMINATION OF TRANSFER LENGTH	52
5.1 End Slip Measurements	52
5.2 Surface Strain Measurements.....	55
CHAPTER SIX - FABRICATION AND TEST SETUP OF FLEXURAL	
SPECIMENS.....	58
6.1 Flexural Specimen Fabrication.....	58
6.2 Flexural Specimen Setup	71
6.2.1 Test Setup.....	71
6.2.2 Loading Conditions	77
CHAPTER SEVEN - FLEXURAL SPECIMEN RESULTS.....	80
7.1 Material Properties	80
7.2 Transfer Length.....	83
7.3 Development Length.....	86
7.3.1 SSB Specimen Flexural Results.....	87
7.3.2 TSB Specimen Flexural Results	93
7.3.3 TB Specimen Flexural Results.....	99
7.3.4 Comparison of Flexural Results.....	103
7.4 VWSG Results.....	105
CHAPTER EIGHT - DESIGN AND FABRICATION OF IT SPECIMENS.....	107
8.1 IT Properties.....	107
8.2 IT Fabrication	113
CHAPTER NINE - IT SPECIMEN RESULTS	118
9.1 Material Properties	118
9.2 Transfer Length Results	118
9.3 Prestress Loss Results.....	120
CHAPTER TEN - CREEP AND SHRINKAGE PRISMS	126
10.1 ACI 209 Creep Model	126
10.2 ACI 209 Shrinkage Model.....	129
CHAPTER ELEVEN - CREEP AND SHRINKAGE PRISM RESULTS.....	131

11.1 Creep.....	131
11.2 Shrinkage.....	134
11.3 Comparison of ACI 209 Prestress Loss Predictions.....	137
CHAPTER TWELVE - SCC BRIDGE MONITORING	140
12.1 Girder Fabrication and Instrumentation	142
12.2 Bridge Layout.....	154
12.3 Bridge Erection	155
CHAPTER THIRTEEN - PRESTRESS LOSS RESULTS OF SCC BRIDGE	169
13.1 Material Properties	169
13.1.1 Girder Properties.....	169
13.1.2 Deck Properties.....	171
13.2 Experimental Stress Results	171
13.2.1 Girders with Conventional Concrete	172
13.2.2 Girders with Self-Consolidating Concrete	176
13.3 Comparison with Code Expressions	179
CHAPTER FOURTEEN - CONCLUSIONS AND RECOMMENDATIONS	186
14.1 Introduction.....	186
14.2 Conclusion Based on Flexural Specimens.....	187
14.3 Conclusions Based on IT Specimens	188
14.4 Conclusions Based on Cowley County Bridge	189
14.5 Recommendations Based on Experimental Results	190
CHAPTER FIFTEEN - IMPLEMENTATION	194
15.1 Recommendations Based on Plant Observations	194
15.2 Recommendations to Evaluate Other SCC Mixtures	195
NOTATIONS	197
REFERENCES	199
APPENDIX	204
A.1 LBPT Tables	204
A.2 Prestress Loss Equations	205
A.3 Shear Calculations for Single Strand Specimens	210
A.4 Nominal Moment Calculations for Single Strand Specimens	211
A.5 Nominal Moment Calculations for TB Specimens	212
A.6 Calculations of Losses for Flexural Specimens	212
A.7 As-Built Dimensions for Flexural Specimens.....	217
A.8 Calculations of Prestress Losses for IT Specimens	218
A.9 Calculation of ACI 209 Prestress Losses for IT specimen	221
A.10 Calculation of Prestress Losses for K3 Girders	223

LIST OF TABLES

Table 1.1 Comparison of Logan and proposed SCC mixture	6
Table 3.2: Properties of different cross sections.....	33
Table 4.1:: LBPT with Logan concrete and project strand	46
Table 4.2: SCC and conventional concrete mixture proportions.....	47
Table 6.1: Review of cast and detensioning dates	59
Table 6.2: Loading conditions for all specimens	79
Table 7.1: Concrete properties of specimens tested	80
Table 7.2: Implied transfer lengths (in inches) for SSB specimens.....	83
Table 7.3: Implied transfer lengths (in inches) for TSB specimens.....	84
Table 7.4: Implied transfer lengths (in inches) for TB specimens	85
Table 7.5: Summary of tested specimens	87
Table 7.6: Comparison of prestress losses for SSB A.....	105
Table 7.7: Comparison of prestress losses for TSB D.....	106
Table 7.8: Comparison of prestress losses for TB A	106
Table 8.1: Geometric properties of IT600	108
Table 9.1: Summary of time-dependent losses	121
Table 9.2: Strand stress predictions at various days	122
Table 11.1: Prestress loss predictions using ACI-209 method	138
Table 11.2: Creep and shrinkage loss predictions using ACI-209 and PCI methods.....	139
Table 12.1: Geometric properties of K3 girder.....	141
Table 13.1: Predicted effective stress values	181
Table 13.4: Prestress loss method using KDOT method for conventional concrete girders	182
Table 13.5: Prestress loss method using ACI/PCI method for SCC girders	182
Table 13.6: Prestress loss method using AASHTO method for SCC girders ...	182
Table 13.7: Prestress loss method using KDOT method for SCC girders	183
Table 13.8: Shrinkage predictions using all five methods.....	185
Table A.1: Mixture proportions stipulated by Logan.....	204
Table A.2: LBPT with SCC and control strand.....	204

Table A.3: LBPT with Logan concrete and control strand.....	205
Table A.4: As-built dimensions for SSB specimens.....	217
Table A.5: As-built dimensions for TSB specimens.....	217
Table A.6: As-built dimensions for TB specimens	217

LIST OF FIGURES

Figure 1.1: Pullout values for conventional concrete versus SCC	5
Figure 2.1: ACI variation of steel stress with distance from free end ⁴	11
Figure 3.1: Cross section of bottom-strand specimens.....	35
Figure 3.2: Cross section of top-strand specimens.....	36
Figure 3.3: Block-out used for top-strand beams.....	37
Figure 3.4: Cross section of T- beam specimen	38
Figure 3.5: Shear reinforcement for T-beams.....	38
Figure 3.6: Crack former in SSB specimens.....	39
Figure 3.7: Crack former for TSB specimen	40
Figure 3.8: Crack former used for TB specimens	40
Figure 3.9: Test setup for 6'-1" embedment length (SSB and TB).....	41
Figure 3.10: Test setup for 6'-1" embedment length for TSB specimens.....	42
Figure 3.11: Test setup for 4'-10" embedment length TSB specimens.....	43
Figure 3.12: Test setup for 4'-10" embedment length SSB and TB specimens ..	44
Figure 4.1: LBPT setup.....	45
Figure 4.2 Inverted slump for SCC	48
Figure 4.3: Ring test for SCC.....	49
Figure 4.4: L-Box test for SCC.....	49
Figure 4.5: Schematic of L-Box (Interim Guidelines, 2003)	50
Figure 4.6: Compressive strength development for SCC	51
Figure 5.1: Making notch on prestressing strand.....	54
Figure 5.2: Measuring distance between notch and steel block	54
Figure 5.3: Whittemore gage	57
Figure 5.4: Whittmore locating points	57
Figure 6.1: VWSGs for SSB A.....	60
Figure 6.2: VWSG for TSB D.....	60
Figure 6.3: VWSGs for TBA	61
Figure 6.4: Digital temperature data logger to record temperature	61
Figure 6.5: SSB bed	62
Figure 6.6: Crack former held in with wood 2 x 4.....	63

Figure 6.7: Pouring of SCC into forms.....	63
Figure 6.8: Finishing of SSB specimens.....	64
Figure 6.9: Cured SSB	64
Figure 6.10: TSB bed with headers in place.....	65
Figure 6.11: Block used to reduce height at mid span.....	65
Figure 6.12 Inserts cast into ends so specimens could be flipped over.....	66
Figure 6.13: Pouring of SCC into forms.....	66
Figure 6.14: Finishing of specimens.....	67
Figure 6.15: Removal of TSB from beds	67
Figure 6.16: Headers spaced for TB specimens.....	68
Figure 6.17: Placement of internal shear stirrups	68
Figure 6.18: Finished shear stirrups in TBs	69
Figure 6.19: Placement of outside walls	69
Figure 6.20: Pouring of SCC into forms.....	70
Figure 6.21: Finishing of top surface	70
Figure 6.22: Torching of strand of TBs	71
Figure 6.23: Carts used for SSB and TSB specimens.....	71
Figure 6.24: Carts for TB specimen.....	72
Figure 6.25: End-slip device used for SSB and TSB	72
Figure 6.26: End-slip device used for TB specimens.....	73
Figure 6.27: LVDTs used for mid-span deflection.....	73
Figure 6.28: Setup used for SSB specimens.....	74
Figure 6.29: Setup used for TSB specimens	74
Figure 6.30: Setup for TB specimens	75
Figure 6.31: Spreader beam for SSB specimens	75
Figure 6.32: Spreader beam used for TB specimens	76
Figure 6.33: Failure for SSB specimen.....	76
Figure 6.34: Failure for TSB specimen.....	77
Figure 6.35: Failure for TB specimen	77
Figure 7.1: Temperature curve during curing for SSB specimen.....	81
Figure 7.2: Temperature curve during curing for TSB specimen	82

Figure 7.3: Temperature curve during curing for TB specimen.....	82
Figure 7.4: Experimental results for transfer length versus other models	86
Figure 7.5: Moment versus deflection for SSB A.....	88
Figure 7.6: Failure of SSB A.....	88
Figure 7.7: Moment versus deflection for SSB C.....	89
Figure 7.8: Failure of SSB C.....	89
Figure 7.9: Moment versus deflection for SSB D.....	90
Figure 7.10: Failure of SSB D.....	90
Figure 7.11: Moment versus deflection for SSB E.....	91
Figure 7.12: Failure of SSB E.....	91
Figure 7.13: Moment versus deflection for SSB F.....	92
Figure 7.14: Failure of SSB F.....	92
Figure 7.15: Moment versus deflection for TSB A.....	93
Figure 7.16: Failure of TSB A.....	93
Figure 7.17: Moment versus deflection for TSB B.....	94
Figure 7.18: Failure of TSB B.....	94
Figure 7.19: Moment versus deflection for TSB C.....	95
Figure 7.20: Failure of TSB C.....	95
Figure 7.21: Moment versus deflection for TSB D.....	96
Figure 7.22: Failure of TSB D.....	96
Figure 7.23: Moment versus deflection for TSB E.....	97
Figure 7.24: Failure of TSB E.....	97
Figure 7.25: Moment versus deflection for TSB F.....	98
Figure 7.26: Failure of TSB F.....	98
Figure 7.27: Moment versus deflection for specimen TB A.....	99
Figure 7.28: Failure of TB A.....	99
Figure 7.29: Moment versus deflection for specimen TB B.....	100
Figure 7.30: Failure of TB B.....	100
Figure 7.31: Moment versus deflection for specimen TB C.....	101
Figure 7.32: Failure of TB C.....	101
Figure 7.33: Moment versus deflection for specimen TB D.....	102

Figure 7.34: Loading of TB D	102
Figure 7.35: Moment versus deflection single strand specimens with 100% I_e	103
Figure 7.36: Moment versus deflection single strand specimens with 80% I_e	104
Figure 7.37: Moment versus deflection for all TB specimens	104
Figure 8.1: Cross section of IT600.....	108
Figure 8.2: VWSG closeup	110
Figure 8.3: VWSGs at mid span	111
Figure 8.4: Load cell at dead end	112
Figure 8.5: Tensioned IT specimen	114
Figure 8.6: Untensioned IT600 specimen.....	115
Figure 8.7: Side-form placement for IT600	115
Figure 8.8: Placement of SCC	116
Figure 8.9: Side-form removal	116
Figure 8.10: Application of Whittemore points	117
Figure 8.11: Flame cutting of strands	117
Figure 9.1: Concrete strain versus specimen length for FT #1	119
Figure 9.2: Concrete strain versus specimen length for FT #2	120
Figure 9.3: Strand stress predictions at various days	123
Figure 9.4: Prestress loss due to shrinkage only	124
Figure 9.5: Concrete strain versus depth for FT #1	125
Figure 9.6: Concrete strain versus depth for FT #2	125
Figure 10.1: Specimen loaded in creep apparatus	128
Figure 10.3: Cylindrical specimen for creep and shrinkage	129
Figure 10.2: Square specimen for creep and shrinkage	129
Figure 11.1: Creep coefficient for square specimens loaded at day one	132
Figure 11.2: Creep coefficient for square specimens loaded at day 28	132
Figure 11.3: Creep coefficient for square and cylindrical (+VWSG) specimens loaded at day one.....	133
Figure 11.4: Creep coefficient for square (+VWSG) specimens at day 28	134
Figure 11.5: Shrinkage strains for square (+VWSG) specimens	135
Figure 11.6: Shrinkage strains for cylindrical (+VWSG) specimens	136

Figure 11.7: Comparison of square versus cylindrical shrinkage strains	137
Figure 11.8: Effective stress versus time for ACI-209 prediction method	138
Figure 12.1: Cross section of K3 girder	141
Figure 12.2: VWSG placement for girders with three gages.....	143
Figure 12.3: VWSG placement for girders with six gages	144
Figure 12.4: Location of VWSG's throughout cross-section	145
Figure 12.5: Location of VWSG's throughout cross-section	146
Figure 12.6: Empty prestressing bed.....	147
Figure 12.7: Tying of internal shear stirrups	148
Figure 12.8: Forms after one side wall has been set into place.....	148
Figure 12.9: Prestressing bed after walls have been set into place.....	149
Figure 12.10: Vibration of conventional concrete mixture	149
Figure 12.11: Laborers not having to vibrate SCC mixture	150
Figure 12.12: Slump test of conventional concrete mixture	150
Figure 12.13: Inverted-slump flow test for SCC mixture	151
Figure 12.14: L-Box test for SCC mixture	151
Figure 12.15: SCC mixture showing no excess paste and presence of aggregate on leading edge.....	152
Figure 12.16: Detensioning of strands with a torch.....	153
Figure 12.17: Presence of "bug" holes in girder with conventional concrete	153
Figure 12.18: Closeup view of "bug" holes in girder w/ conventional concrete .	153
Figure 12.19: Smooth exterior of SCC girder	154
Figure 12.20: Closeup of smooth SCC finish.....	154
Figure 12.21: Layout and designation of bridge girders.....	155
Figure 12.22: One lane open to traffic during phase I construction	156
Figure 12.23: Temporary supports for existing bridge	157
Figure 12.24: Placement of cages for piles	157
Figure 12.25: Abutment wall.....	158
Figure 12.26: Placement of girders.....	158
Figure 12.27: Underneath view of placed girders	159
Figure 12.28: Underneath view of placed girders	159

Figure 12.29: Placement of shoring for deck casting	160
Figure 12.30: Placement of shoring for deck casting-II.....	160
Figure 12.31: Placement of deck reinforcement	161
Figure 12.32: Tying of deck reinforcement into place	161
Figure 12.33: Wires extending into multi-plexor.....	162
Figure 12.34: Wires extending through abutment wall.....	162
Figure 12.35: Pump truck for pumping concrete to bridge deck	163
Figure 12.37: Finishing of concrete	164
Figure 12.38: Opened lane of phase I and beginning of phase II	165
Figure 12.39: Groundwork for phase II	165
Figure 12.40: Shoring for phase II	166
Figure 12.41: Deck completion of phase II	166
Figure 12.42: Finished bridge and approach	167
Figure 12.43: Side restoration	167
Figure 12.44: Solar panel on side railing	168
Figure 12.45: Side view of completed project.....	168
Figure 13.1: Modulus of elasticity for girders gaged with VWSGs	170
Figure 13.2: Compressive strength for girders gaged with VWSGs.....	170
Figure 13.3: Release compressive strength for all girders cast	171
Figure 13.4: Effective stress for girder A3	172
Figure 13.5: Effective stress for girder B1	173
Figure 13.6: Effective stress for girder B3	173
Figure 13.7: Effective stress for girder C3	174
Figure 13.8: Concrete versus depth for girder A3.....	174
Figure 13.9: Concrete versus depth for girder B1.....	175
Figure 13.10: Concrete versus depth for girder C3.....	175
Figure 13.11: Effective stress for girder D1	176
Figure 13.12: Effective stress for girder D3	177
Figure 13.13: Effective stress for girder E3	177
Figure 13.14: Strain versus depth for girder D1.....	178
Figure 13.15: Strain versus depth for girder D3.....	178

Figure 13.16: Strain versus depth for girder E3	179
Figure 13.17: Comparison of SCC vs conventional concrete effective stress ..	180
Table 13.2: Prestress loss ACI/PCI method for conventional concrete girders	181
Table 13.3: Prestress loss AASHTO method, conventional concrete girders ...	181
Figure 13.18: Effective stress calculations for conventional concrete girders...	183
Figure 13.19: Effective stress calculations for girders with SCC.....	184
Figure 13.20: Effective stress comparison w/ five methods, girders with SCC .	185
Figure 14.1: Block #1.....	191
Figure 14.2: Block #2.....	192
Figure 14.3: Block #3 (Loaded with 1400 pounds)	192

CHAPTER ONE - INTRODUCTION

Self-consolidating concrete (SCC) has rapidly become a widely used material in the construction industry. SCC is defined as a highly workable concrete that can flow through densely reinforced or geometrically complex structural elements under its own weight, and adequately fill voids without segregation or excessive bleeding without the need for vibration. The workability can be characterized by the following properties (Interim Guidelines, 2003).

- Filling ability: the ability of SCC to flow under its own weight into all spaces in the formwork.
- Passing ability: the ability of SCC to flow through openings close to the size of the coarse aggregate without segregation or aggregate blocking.
- Stability: the ability of SCC to remain homogeneous during transport and placing, and after placement.

The “Interim Guidelines for the Use of Self-Consolidating Concrete in PCI Member Plants” recommends that “strand bond tests shall be run with new SCC mixes to verify that the bond with SCC is equivalent or better than a conventional concrete of similar design when using similar strand.” These guidelines state that “this can be done using a flexural development length test or by direct load testing.” Because SCC does not require any external vibration during placement, some design engineers have expressed concern about its ability to achieve adequate bond with the strand.

At the onset of this research program very few studies had been conducted to evaluate the bond strength between the prestressing strand and SCC. Most of the current research on SCC had been focused on development of SCC mixtures,

comparisons of hardened concrete properties of SCC mixtures to conventional (needing vibration) concrete and testing methods for evaluation of fresh SCC mixture. As summarized in the literature review (Chapter Two), most studies on bond have been done with conventional concrete (CC) and those done with SCC have had highly inconclusive results. In addition to the lack of data about SCC and bond, a concern also exists on the long-term performance of pretensioned, prestressed bridge girders cast with SCC. This manuscript will address the issues of bond and time-dependent deformations associated with long-term prestress losses for prestressed bridge girders containing SCC.

1.1 Background

The Kansas Department of Transportation (KDOT) would like to use SCC in pretensioned bridge members to enhance the aesthetics and improve consolidation in congested areas. Kansas precasters want to use this type of concrete for a variety of reasons. A drawback with conventional concrete is that, in hard to vibrate areas such as the flange of inverted T-shape members, air is trapped at the surface of the form producing “bug” holes. SCC will help ensure proper consolidation and improve the finish on these surfaces.

However, before allowing the use of SCC in state bridge girders, KDOT wanted to investigate the bond and flexural characteristics of an SCC mixture proposed by the local precaster, Prestressed Concrete Inc, in Newton, Kansas. Prestressed Concrete Inc developed their proposed SCC mixture proportions with the help of their admixture supplier. Because SCC is placed without external vibration, KDOT was concerned that the bond between the SCC and strand may not be as strong as that achieved with a

conventional concrete mix. At the onset of this study, information about the transfer and development lengths of prestressing steel in SCC, and the applicability of the American Concrete Institute (ACI) and American Association of State Highway Transportation Officials (AASHTO) equations to these members were essentially absent from the literature.

Transfer length is the distance required to transfer the fully effective prestressing force from the strand to the concrete. Development length is the bond length required to anchor the strand as it resists external loads on a member. (Russell, 1993) As external loads are applied to a flexural member, the member resists the increased moment demand through increased internal tensile and compressive forces. Increased tension in the strand is achieved through anchorage to the surrounding concrete (Peterman, 2000). Transfer and development length are defined in detail in Chapter Two of this manuscript.

Current American Concrete Institute Building Code Requirements (ACI 318-05, 2002) and American Association of State Highway Transportation Officials (AASHTO, 2004) design requirements do not specifically address the use of SCC in prestressing applications. The ACI 318 and AASHTO expressions for transfer and development lengths are based on tests performed with conventional concrete (CC) and are as follows:

Transfer length (L_{tr}):

$$L_{tr} = \frac{f_{se}}{3} d_b \quad (1.1)$$

Development length (L_{dev}):

$$L_{dev} = \left(f_{ps} - \frac{2}{3} f_{se} \right) d_b \quad (1.2)$$

where

d_b = diameter of strand in inches;

f_{se} = effective stress in prestressing strand after allowance of prestress losses (ksi); and

f_{ps} = stress in prestressing strand at calculated ultimate capacity of section (ksi).

The AASHTO, 2004 specifications require an additional 1.6 multiplier to equation 1.2 for precast, prestressed beams.

The Kansas Department of Transportation (KDOT) funded an initial investigation in which large-block pullout tests (Logan, 1997) (LBPTs) were performed at Kansas State University (KSU), using both the standard concrete recommended by Logan and the proposed SCC mix, Table 1.1. The concrete compressive strength of the Logan mixture was 5,600 psi and 6,800 psi for the SCC mixture. The results with SCC had both lower first-slip and ultimate-load values compared to those values when the Logan concrete was used (Tables A.2 and A.3). A comparison of the values for both the conventional concrete and SCC mixtures are shown in Figure 1.1. Note, Logan recommends that all 0.5-inch strand should have an average minimum pullout capacity of 36 kip, with a maximum coefficient of variation of 10% for a six-sample group. Logan has since added an additional recommendation that the minimum average value of first-observed slip of 0.5-inch strand should be 16 kip. Furthermore, the values with SCC were below the values of 16 kip and 36 kip for first-observed slip and maximum pullout force, respectively. Both of these LBPTs used strand from the same unweathered reel, which had exhibited satisfactory bond performance in flexural beam tests. This strand is referred to as the control strand.

Based on these initial pullout results, it was determined that full-scale, development length girder tests were necessary to further investigate the bond between SCC and the prestressing strand. Thus, KDOT funded an experimental program to evaluate the flexural performance of pretensioned concrete members with the proposed SCC mixture.

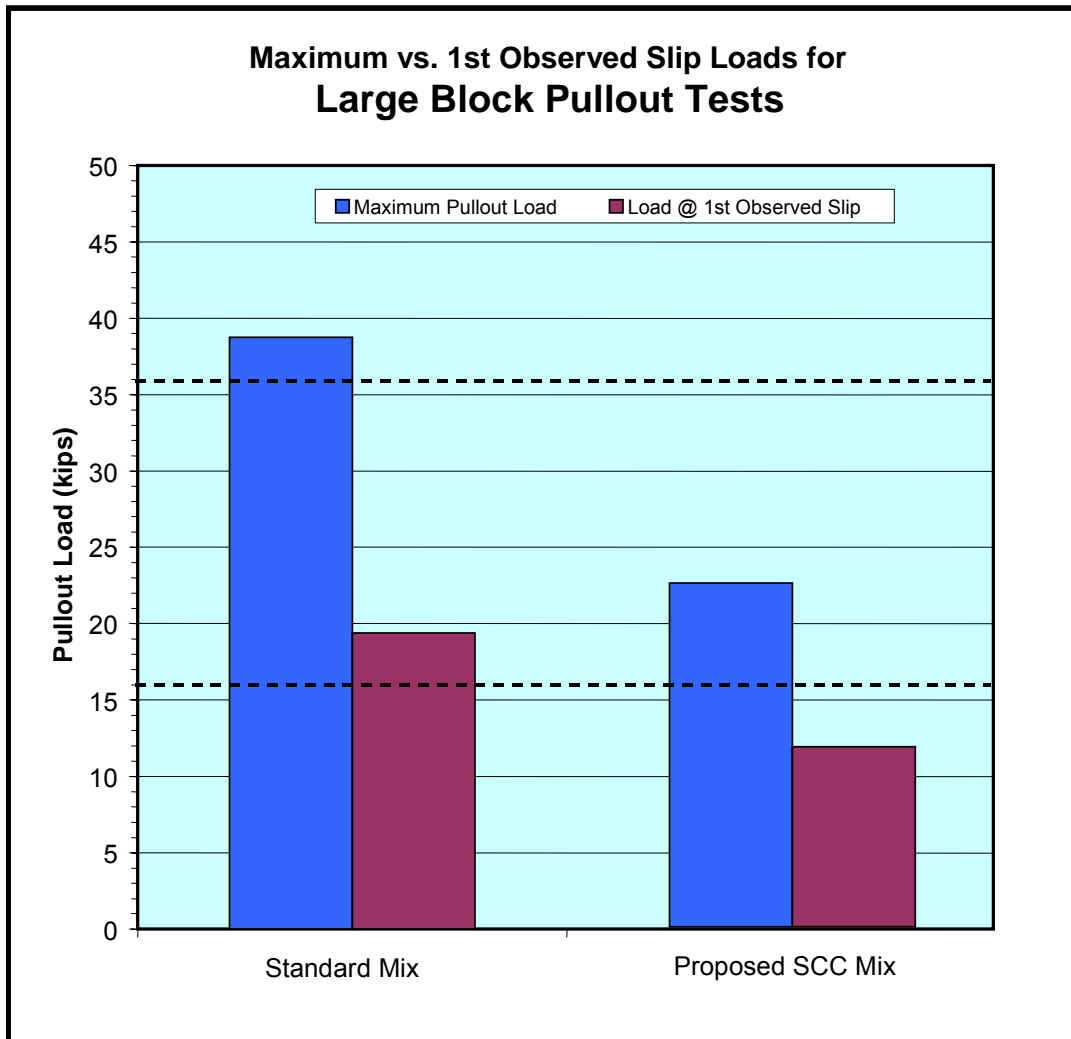


Figure 1.1: Pullout values for conventional concrete versus SCC

Table 1.1 Comparison of Logan and proposed SCC mixture

Materials	Logan	SCC
Cement (Type III)	660 lbs	750 lbs
3/4" Max Limestone	0 lbs	1360 lbs
3/4" Max Crushed Gravel	1900 lbs	0 lbs
Concrete Sand	1100 lbs	1360 lbs
HRWR (ASTM C 494 Type F)	0 oz	70 oz
Normal Range WR (ASTM C 494 Type A)	26 oz	0 oz
Air-entraining agent (ASTM Designation C260)	0 oz	5 oz
Water	35 gal	27 gal

1.2 Test Program

1.2.1 Overview of Experimental Program

Girders were cast with different cross sections and embedment lengths to test the flexural capacities of these different configurations. Single-strand, top-strand, and multiple-strand girders were all cast and tested.

1.2.1.1 Transfer Length

Transfer lengths were estimated for 16 specimens by measuring strand end-slip at each specimen end. The SCC mix design and prestressing strand reel were constant for all specimens, with the primary variables being the number of strands and the location of the strand from the bottom of the specimen.

1.2.1.1 Development Length

A series of development length tests were performed on the flexural specimens that were cast. Specimens were tested with embedment lengths equal to that of development lengths (L_{dev}) predicted by code equations. Specimens with embedment lengths of 80% of L_{dev} were also tested.

1.2.2 Inverted-T-Shape Specimens

Specimens with an Inverted-T (IT) shaped cross-section were cast in order to determine time-dependent deformations. The IT section was chosen because KDOT is beginning to use this section more in their bridges. Elastic shortening, creep, and shrinkage losses were determined from experimental results. In addition, companion creep-and-shrinkage prisms were cast in order to compare with current ACI code recommendations.

1.2.3 Cowley County Bridge

Thirty-five bridge girders were cast and placed in the field to analyze combined creep and shrinkage effects of SCC. Of these 35 girders, 14 were cast with SCC and the remaining 21 with conventional concrete. Vibrating wire strain gages were embedded in seven of the girders to record these time-dependent deformations. The bridge is located in Cowley County, approximately five miles west of Winfield, Kansas, on US Highway 160.

1.3 Scope

Chapter Two presents a literature review of past research completed and defines key terms.

Chapter Three addresses different types of girders used in the flexural specimen test program.

Chapter Four discusses material properties of prestressing strand and concrete, along with different test methods used to evaluate fresh concrete properties.

Chapter Five presents methods for measuring transfer length in the development length girders and inverted-T-shape specimens.

Chapter Six shows fabrication, loading conditions, and test setup configurations for the flexural specimens.

Chapter Seven presents transfer and development length results of the flexural specimens.

Chapter Eight gives the properties of the inverted-T-shape section used for determining creep and shrinkage properties.

Chapter Nine shows results yielded from the inverted-T-shape section. These results include both transfer length and prestress losses.

Chapter Ten presents the setup for the creep-and-shrinkage prisms, along with code equations.

Chapter Eleven gives results for the creep-and-shrinkage prisms, along with comparisons with ACI 209 design recommendations.

Chapter Twelve shows fabrication of the girders used for the bridge that was instrumented with strain gages, along with the erection process of the bridge.

Chapter Thirteen presents prestress loss results of the girders from the bridge that was instrumented.

Chapter Fourteen presents conclusions and recommendations resulting from this project.

CHAPTER TWO - BACKGROUND & LITERATURE REVIEW

2.1 Prestressed Concrete

2.1.1 Concepts

Prestressing can be defined as the preloading of a structure, before the application of service loads, so as to improve its performance in specific ways.(Nilson, 1987)

Concrete is widely regarded as a compression material. The idea of prestressing is to take full advantage of this material property. The original concept of prestressing concrete was to introduce sufficient axial precompression in beams so that all tension in the concrete was eliminated at service load (Nilson, 1987). The following equation is used to analyze stresses in the prestressed member:

$$f_c = \frac{P}{A} \mp \frac{P \cdot e \cdot y}{I} \pm \frac{M \cdot y}{I} \quad (2.1)$$

where

f_c = stress at a given point;

P = prestressing force;

e = eccentricity (distance from the geometric centroid of the beam to geometric centroid of the steel);

I = moment of inertia;

y = distance from centroid of the cross section to the point in question; and

M = moment due to applied external loads.

There are two common methods to prestress concrete: pretensioning and post-tensioning. For the purpose of this research, only pretensioned concrete members will be examined. The general process of pretensioning has the following characteristics:

- Uses a bed.
- Strand is tensioned first.
- Concrete is cast around the strand.

- Strand is cut after a time period allowing the concrete to harden, transferring prestressing force by bond.
- Some prestressing force is lost because the concrete shortens elastically under released prestressing load and the strand shortens along with it.

Prestressed concrete is heavily dependent on the bond between prestressing strands and concrete. This bond is thoroughly investigated in this study.

2.1.2 Definitions

In this section, transfer length, development length, and embedment length are defined. A list of other terms used throughout this manuscript are shown in the Notations section.

Transfer length (L_{tr}) is the distance required to transfer the fully effective prestressing force from the strand to the concrete. In other words, transfer length is the length of bond between the free end of the strand, where there is zero stress, to the point where the prestressing force is fully effective. Strand tension increases due to bond stresses that restrain or hold back the strand. The idealized stress in the prestressing strand along the length of the specimen is shown in Figure 2.1, where both transfer length and development length regions are labeled. This diagram is the ACI assumed variation of steel stress.

Development length (L_{dev}) is defined as the bond length required to anchor the strand as it resists external loads on the member. In the case where the bonded length exceeds the development length, while the member is under external loads, then strand tension has adequately developed and bond length is sufficient. However, if the bonded

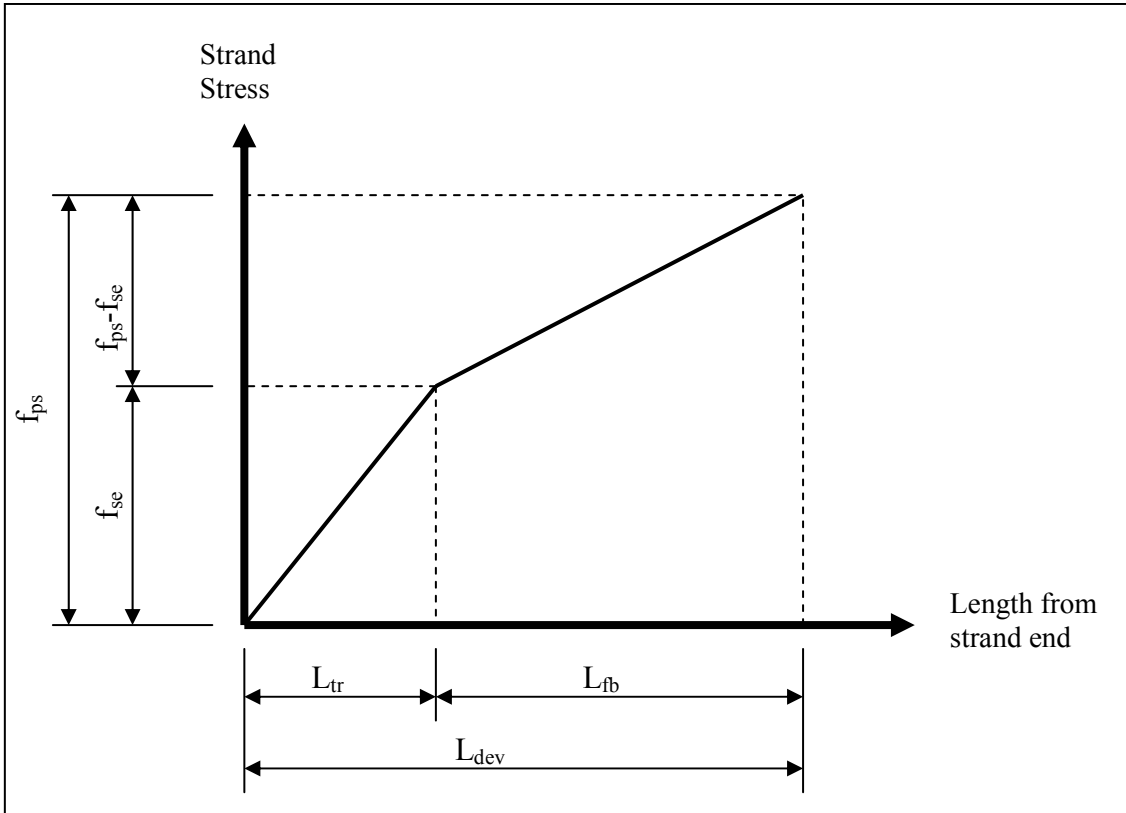


Figure 2.1: ACI variation of steel stress with distance from free end⁴

length of the strand is less than the development length, then strand slip occurs throughout the concrete while under the influence of external loads.

Embedment length (L_e) is defined as the length of bond from the critical section to the beginning of bond. The critical section is located where the steel stress is at its maximum point, usually the point of maximum moment. The beginning of bond usually occurs at the end of a fully bonded member. In order to prevent bond failure, embedment length must be equal to or greater than development length.

2.1.3 Prestress Loss Equations

ACI 318 (ACI 318, 2002), AASHTO LRFD Bridge Design Specifications (AASHTO LRFD, 2004), KDOT (KDOT Design, 2003), and The PCI Design Handbook (PCI, 2004) all have slight differences in determining losses of prestressed members. Each method

is detailed in section A.2. The ACI 209 Committee¹⁰ procedure for determining prestress losses is also shown. This method uses creep coefficient and shrinkage strains resulting from laboratory tests.

2.2 Self-Consolidating Concrete

Self-consolidating concrete was first developed in Japan in the mid-1980s. Ouchi (Ouchi, 2001) reports that durability of concrete structures was a major topic of interest in Japan. One of the key components of making durable concrete is to have proper compaction. However, getting this proper compaction was becoming a major concern because the number of skilled workers in Japan was declining, thus leading to the deficient structures. A solution to this lack of proper compaction by skilled workers was to develop a concrete that could be compacted into every corner of formwork purely by means of its own self-weight and without the need for vibrating compaction.

SCC gets its flowable properties from admixtures that are added to the concrete. Bury and Christensen (2003) describe how the admixtures give the concrete its fluid characteristics. The high-range water-reducing (HRWR) admixtures, as defined by ASTM C494, allow the concrete to remain stable during and after placement, along with a high degree of workability. HRWR admixtures allow improved cement dispersion over older, water-reducing admixtures. According to Bury and Christensen HRWR admixtures impart a negative charge on the cement particles, causing them to repel from one another. In addition, admixtures have side chains of varying lengths, which are engineered to be part of the backbone of the molecule and help keep the cement particles apart. This allows more water to surround more surface area of the cement

particles. The dual action of the admixtures allows for improved cement dispersion, more complete hydration of the cement, and improved workability (Bury and Christensen, 2003).

Ouchi et al. (2003) completed a study in which applications of SCC in Japan, Europe and the United States were examined. Japan has been using SCC in large quantities since the early 1990's and within the last 6-8 years Europe has constructed a number of bridges with SCC while the main use of SCC in the U.S. is still mainly for architectural concrete. One of the major differences between the SCC being produced in Japan and Europe as compared to the SCC produced in the U.S. is the improved bond quantity of the SCC in Japan and Europe. Ouchi et al. report that in general the SCC bond strength when expressed in terms of compressive strengths are higher with SCC than with conventional concrete.

2.3 Elements of Bond

This section details the past research that has been completed on the subject of bond (transfer and development length) between prestressing strand and concrete. Most of the research has been completed with conventional concrete, as only recently has SCC been used in prestressed concrete members.

Janney (1954) completed one of the first studies of bond in pretensioned, prestressed concrete girders. Prismatic specimens were used to study the bond near the end of the prestressed member. Beam specimens were also used to study flexural bond and the interrelation between flexural bond and the resulting bond from the transfer of prestress. Several variables were considered, which included strand

diameter and surface condition. The study was set out to answer the following questions:

- To what extent does wire diameter influence transfer of pretension from steel to concrete?
- How are prestress transfer bond properties of wire and strand influenced by surface conditions?
- What is the effect of concrete strength on the transfer of stress from pretensioned steel to concrete?

Janney concluded that strand diameter size used in the study will result in sufficient strength through bond. Also, the transfer bond is a large function of the friction between the concrete and steel. The author noted that results were only taken after release and did not take into account the effect of time, fatigue, and impact.

Hanson and Kaar (1959) carried out an investigation of flexural bond on 47 prestressed beams. The principal factor investigated was variation of strand embedment length with different strand diameters. Strand surface condition, reinforcement percentage, and reduction in concrete strength were also investigated in a limited manner. It was found that strand with a rusted surface condition did exhibit better bond. The following design guidelines were proposed:

- Calculate steel stress at ultimate flexural strength, assuming that no general bond slip occurs.
- Check embedment length of strand, that is, the distance from the free end of the strand to the section of maximum steel stress.

- From given charts, determine maximum steel stress that can be developed in the embedment length provided for the chosen size of strand.

Kaar et al. (1963) investigated the influence of concrete strength on transfer length at the time of release over a one-year period. Rectangular, concentrically prestressed members fabricated with different concrete strengths and strand diameters were used in this investigation. Surface strains measured by a Whittemore gage, were used to determine transfer lengths of each specimen. Immediately before transfer, and then at 1, 3, 7, 14, 28, 56, 90, 180, and 365 days, readings were taken. The authors concluded that

- concrete strengths at transfer of prestress had little influence on the transfer lengths;
- for specimens using strand up to 0.5-inch in diameter, transfer lengths measured adjacent to the flame-cutting end were approximately 20 percent greater than transfer length at the opposite end;
- for 0.6-inch-diameter strands, transfer length increase was 30 percent;
- average increase in transfer length over a period of one year following prestress transfer was 6 percent; and
- increase in transfer length with time was independent of concrete strength at the time of transfer.

Janney (1963) evaluated stress-transfer characteristics of a new type of prestressing strand that had a higher minimum breaking strength than previously used strand. Six specimens were cast and tested. Two were prestressed with conventional 0.5-inch-diameter clean and bright strand. Two other specimens were prestressed with

0.5-inch-diameter clean and bright high strength strand. Finally, the remaining two specimens were prestressed with 0.5-inch-diameter, high-strength strand with a medium coat of rust over the surface. The test specimens were 3.5 inches (H) by 4.25 inches (B) and eight feet in length. Each member was prestressed with a single prestressing strand located at the centroid. Mechanical gage points were mounted on the concrete surface, and resulting compressive strains were used in determining transfer lengths. Results yielded a slightly greater transfer length for the specimens with high-strength strand. However, the author argues that this slight increase should not be significant from a design standpoint.

Kaar and Hanson (1975) completed a study in which 108 pretensioned concrete beams were tested under cyclic loading, simulating the loads sustained by a railroad crosstie. Repeated loads were applied to one of the four selected locations near the end of the beam. The load used was one that would open the crack 0.001 inches or 15% greater than the crack-opening load. Different surface conditions of strand and release of prestress were also evaluated. The authors concluded that the load cannot be applied nearer than 2.2 times the strand transfer length for smooth 3/8-inch diameter strand to obtain a bond-fatigue life of more than 3 million cycles. The authors also concluded that these railroad ties should be constructed with short transfer lengths and to decrease transfer lengths, the strand should be roughened without reducing its diameter.

Martin and Scott (1976) presented equations for designing precast, pretensioned members for spans too short to provide an embedment length enough to develop the

full strength of the strand. Test results obtained from Hanson and Kaar (1959) were used in developing their equations. For embedment lengths less than $80d_b$

$$f_{ps} \leq \frac{l_e}{80d_b} \left(\frac{135}{d_b^{1/6}} + 31 \right) \quad (2.2)$$

and for embedment lengths greater than $80d_b$

$$f_{ps} \leq \frac{135}{d_b^{1/6}} + \frac{0.39l_e}{d_b} \quad (2.3)$$

where

f_{ps} = stress in prestressing strand at calculated ultimate capacity of section (ksi);
 d_b = diameter of strand in inches;
 l_e = embedment length in inches.

Also, f_{ps} shall not be greater than the results given by strain compatibility.

The investigation conducted by Zia and Mostafa (1977) centered on developing new equations for both transfer and development lengths. Previous research found that transfer length can be affected by a large number of parameters including

- type of steel (wire or strand)
- steel size (diameter)
- steel stress level
- surface condition of steel (clean, oiled, rusted)
- concrete strength
- type of loading (static, repeated, impact)
- type of release (gradual, sudden (flame cutting, saw-cutting))
- confining reinforcement around steel (helix or stirrups)
- time-dependent effect
- consolidation and consistency of concrete around steel

- amount of concrete coverage around steel

After analyzing all transfer length results that were tabulated, the authors came up with new equations for both transfer and development length.

$$L_t = 1.5 \frac{f_{si}}{f_{ci}} d_b - 4.6 \quad (2.4)$$

$$L_{dev} = 1.5 \frac{f_{si}}{f_{ci}} d_b - 4.6 + 1.25(f_{su} - f_{se}) d_b \quad (2.5)$$

The equation for transfer length is applicable for concrete strength ranging between 2,000 and 8,000 psi. This expression formulated by the authors takes into account the effect of strand size, initial prestress, and concrete strength at release. In addition, the equations are conservative from the actual lengths that were observed and would make a suitable transfer length for the ACI expression.

Cousins et al. (1990) present development of analytical equations for transfer length and flexural bond lengths for prestressed members. Experimental results gathered from previous work were used in deriving these equations. The suggested equation for transfer length is

$$L_t = 0.5 \left(\frac{U_t' \sqrt{f_{ci}'}}{B} \right) + \frac{f_{se} A_s}{\pi d U_t' \sqrt{f_{ci}'}} \quad (2.6)$$

where recommended values of U_t' are 6.7 for uncoated strand, 10.6 for coated strand with low grit, and 16.5 for strand coated with medium to high grit. The value of B , the bond modulus, had an average value of 300 psi/in and used for equation 2.6. The equation for flexural bond lengths was suggested as

$$L_{fb} = (f_{ps} - f_{se}) \left(\frac{A_s / \pi d}{U_d' \sqrt{f_c'}} \right) \quad (2.7)$$

where the recommended values of U_d' are 1.32 for uncoated strand, 6.40 for coated strand with medium to high density of grit, and 4.55 for coated strand with low-density grit. Finally, the development length is just the sum of the proposed equations for transfer and flexural bond length ($L_t + L_{fb}$).

Cousins et al. (1992) present a method for evaluating the bond of prestressing strand to concrete. The purpose of this research was to develop a standard test for determining bonding characteristics of prestressing strand to concrete and to correlate the test to transfer length. An experimental program was conducted to compare transfer lengths of the proposed test to a direct tension pullout test. The authors concluded that the proposed standard test was simple and easy to perform. Plus, test results were very similar to those obtained from direct tension pullout tests.

Shahawy et al. (1992) conducted an investigation in which full-scale pretensioned AASHTO girders were examined for transfer length. Different prestressing strand diameter sizes were used. Concrete surface strains were used in determining the transfer length of each girder. Results showed that ACI/AASHTO predictions for transfer length were inadequate. The authors showed that if f_{si} was used instead of f_{se} , a much better comparison between experimental transfer length and results from using code expressions exist. They recommend this change be made for the ACI/AASHTO expression for transfer length.

Mitchell et al. (1993) cast 22 pretensioned concrete beam specimens to determine the influence of concrete strength on transfer and development lengths. The two main variables in this study were concrete strength and strand diameter. Concrete compressive strengths varied from 3,050 to 7,250 psi at transfer to 4,500 to 12,900 psi

at time of testing. Strand diameters used in the specimens were 0.375 inches, 0.5 inches, and 0.62 inches. Concrete surface strains were used to assess transfer lengths. Strain measurements were taken before release, just after release, and just prior to testing. Test results showed that an increase in concrete strength gives smaller transfer lengths. The following equation for transfer length was derived from the experimental data:

$$L_t = 0.33 f_{pi} d_b \sqrt{\frac{3}{f_{ci}}} \quad (2.8)$$

The following equation for development length was derived:

$$L_{dev} = 0.33 f_{pi} d_b \sqrt{\frac{3}{f_{ci}}} + (f_{ps} - f_{se}) d_b \sqrt{\frac{4.5}{f_c}} \quad (2.9)$$

Alternatively a simpler, more conservative expression for transfer length was also recommended:

$$L_t = 50 d_b \sqrt{\frac{3}{f_{ci}}} \quad (2.10)$$

This expression can be conservatively used in checking stresses but should not be used to calculate the transfer length component of the development length.

Buckner (1995) summarizes FHWA's independent review of design recommendations for transfer and development length. The objectives of the study were to

- conduct a review of literature related to strand transfer and development length research;
- analyze data from recent studies and rationalize discrepancies among conclusions drawn from those studies; and

- recommend equations for strand transfer and development length consistent with current practices.

The author recommends the following equation be used for transfer length:

$$L_t = \frac{f_{st}d_b}{3} \quad (2.11)$$

Also, for strands either straight or draped that have more than 12 inches of concrete cast beneath the strand, transfer length should be multiplied by 1.3. These recommendations apply only to Grade 270, seven-wire, low-relaxation uncoated strand used in pretensioned members with normal-weight concrete having compressive strengths at release of 3,500 psi or higher. The study also recommends a conservative expression for development length:

$$L_{dev} = \frac{f_{st}d_b}{3} + \lambda(f_{ps} - f_{se})d_b \quad (2.12)$$

where for general application, the multiplier λ is taken as $(0.6+40\lambda_{ps})$. For λ it shall be taken greater than or equal to 1.0 and less than or equal to 2.0. As was the case in the transfer length expression, if more than 12 inches of concrete is below the strand, the development length expression should be multiplied by 1.3.

Martin and Korkosz (1995) present a strain compatibility method for calculating nominal flexural capacity for sections in which the strand is not completely developed. This is critical at the ends of members where strands may be debonded to reduce release stresses. The authors contend that in short-span members, the prestressing strand may not be fully developed at sections of high moment and this could cause a premature failure. Equations are presented in which concrete strains are used in determining the nominal flexural capacity. They also recommend that the strength-

reduction factor of $\phi = 0.85$ be applied to the calculated nominal-moment strength, when the failure end point is strand slip.

Russell and Burns (1996) conducted a study in which transfer lengths were measured and compared to the current AASHTO and ACI code provisions. A wide variety of research variables were used in conducting this research, including

- number of strands (1, 3, 4, 5, and 8),
- size of strand (0.5 and 0.6 inch diameter),
- debonding (fully bonded or debonded strands),
- confining reinforcement (with or without), and
- size and shape of the cross section.

A total of 44 specimens were tested and transfer lengths were measured on both ends of the specimens. Transfer lengths were measured using concrete surface strains along the length of each specimen. End slips and use of electrical-resistance strain gages were also used in determining transfer lengths. Resulting data confirms the current code expressions that transfer length varies proportionately with strand diameter. It was also found that transfer length is not a linear, but rather that transfer length is an exponential function of strand diameter. Another relationship found in this study was that test specimens with a larger cross sections and multiple strands possess significantly shorter transfer lengths. Strand end slips were also used to find a correlation between end slip and transfer length. The equation

$$L_t = 294.4L_{es} \quad (2.13)$$

where

$$L_{es} = \text{measured end slip (inch)}$$

was derived from the data by performing a regression analysis. The reported correlation of $r = 0.717$ indicates that a good correlation exists between transfer length and strand-end slip. It was also found that confining reinforcement had little or no effect in lessening transfer lengths. A safe expression for transfer length was derived:

$$L_t = \frac{f_{se} d_b}{2} \quad (2.14)$$

This expression is proposed to be used in all design considerations.

Rose and Russell (1997) sought to evaluate three different bond-performance tests and their potential to predict bond characteristics. Simple pullout tests, tensioned pullout tests, and measured strand-end slips were compared to companion transfer lengths with varying surface conditions. It was concluded that strand-end slips provide a reliable indication of transfer length. It was found that the theoretically derived expression

$$L_t = 2L_{es} \left(\frac{E_{ps}}{f_{st}} \right) \quad (2.15)$$

can reliably predict transfer length. The research demonstrates that strand end slip is the most reliable assessment of bond performance when compared to simple and tensioned pullout tests. Use of strand end slip was found to be independent of strand surface conditions. They found that a roughened surface enhances bond, whereas a lubricated surface hinders bond performance. Also it was noted that transfer lengths can increase as much as 60 percent when adjacent to flame cutting.

Logan (1997) wrote an extensive paper on the acceptance criteria for bond quality for prestressed concrete applications. This paper also addressed the procedure for performing large-block pullout tests and requirements for these tests. For this study,

prestressing strand was collected from a wide variety of places throughout the country to evaluate strand-bond performance. More than 200 tests were conducted on specimens that included large-block pullout tests, end slip at release and 21 days, and development length tests. The author concluded that the large-block pullout tests are an accurate predictor of general transfer and development length characteristics of the strand in prestressed concrete applications. The author also concluded, that based on the results of the large-block pullout tests, one can determine if the transfer and development length equations predicted by ACI will pass. It was also concluded that there are high-bond quality and poor-bond quality strands in the marketplace. Initial end-slip measurements do not detect poor-bonding strand; however, end-slip values at 21 days do provide a warning of potential bond problems. Residue that comes off during a wipe test provides no indication of subsequent bond performance.

Lane (1998) introduce new development and transfer length equations after a long study performed by the Federal Highway Administration (FHWA). The research was brought on by a 1988 Memorandum issued by the FHWA which disallowed the use of 0.6 inch diameter strands in pretensioned applications, restricted the minimum center-to-center strand spacing to four times the nominal diameter of the strand, and increased the required development length for fully-bonded and debonded strands by 1.6 and 2.0 times AASHTO Equations 9.32 (Equations 1.1 and 1.2 in this manuscript). The memorandum was only an interim measure until further research could be conducted and AASHTO adopted the new regulations. In 1996 the memorandum was changed due to the results of new research and the use of 0.6 inch diameter strand was allowed and the spacing of strands was returned to their original values. During this time the

FHWA also conducted a study to evaluate and introduce a new equation for both development and transfer length. The study consisted of measuring the development and transfer length of different prestressed members. After analyzing their experimental results and reviewing the work of many others, the FHWA produced the following equations for transfer and development length and that a 1.3 multiplier be applied for any strand (straight or draped) in any member that has 12 inches or more of concrete cast below the strand.

$$L_t = \frac{4f_{pt}D}{f'_c} - 5$$

$$L_d = \left[\frac{4f_{pt}D}{f'_c} - 5 \right] + \left[\frac{6.4(f_{su}^* - f_{se})D}{f'_c} + 15 \right]$$

where

f_{pt} = stress in prestressing strand prior to transfer of prestress (ksi);
 D = nominal diameter of prestressing strand (inch);
 f'_c = concrete compressive strength at 28 days (ksi);
 f_{su}^* = average stress in prestressed reinforcement at ultimate load (ksi); and
 f_{se} = effective stress in prestressed reinforcement after all losses (ksi).

Peterman et al. (2000) conducted a study in which 18 development length tests were carried out on single-strand, rectangular and multiple-strand, T-shaped specimens. Concrete used in this study was semi-lightweight. Transfer lengths of the specimens tested were also conducted by measuring concrete surface strains. Results from transfer lengths yielded values that were less than AASHTO and ACI code provisions for shear, except in one case where splitting of concrete was noted. In rectangular beam tests, all specimens exceeded their design-moment capacities. However, in the T-beams, bond failures at loads below the design capacity occurred in some of the specimens. Failure occurred due to a flexure-shear crack near the loading

point. The authors then conducted further tests and recommended that current AASHTO and ACI requirements for strand-development length be enforced at a critical section located a distance d_p from the point of maximum moment towards the free end of the strand. An alternative solution was noted that the designer may elect to provide enough transverse reinforcement to minimize the shift in tensile demand that will occur in the event of diagonal cracking.

Steinberg et al. (2001) conducted an experimental study in which concrete strains of three pretensioned concrete beams were monitored. The strains were evaluated through use of electrical-resistance strain gages embedded in the beam and surface mounted to the beams. Transfer lengths were determined by concrete strains and by strand end slip. The researchers concluded that the manual method (concrete surface strains) provided comparable values to the end-slip method. Results also showed that longitudinal tensile strains existed near the end of the beams prior to cutting all the strands. These strains were large enough to cause cracking, which was not visible after release of all the strands.

Oh et al. (2001) completed a comprehensive experimental program in which they compared current ACI design code for transfer length against experimental results. Major variables focused on were strand diameter, concrete strength, concrete cover size and strand spacing. Their results showed that as transfer length decreases with an increase in concrete strength, it also decreases with an increase in concrete cover. Transfer lengths were determined using both concrete surface strains and strand end slip. It was found that a good correlation exists between measuring transfer lengths by strand end slip and concrete surface strains. The author concluded the following:

- The current ACI code equation for transfer length overestimates actual measured transfer lengths.
- Transfer length increases with an increase in strand diameter; however, the ACI code expression assumes this relationship to be linear and experimental results do not support this.
- Transfer lengths tend to increase slightly with time due to creep effects and the increase of transfer length is about 5% at 90 days after prestress transfer.
- The ACI code expression for transfer length should include concrete strength and concrete cover size.

Barnes et al. (2003) conducted a study on 36 full-scale, development length girders. Girders cast each had a unique strand surface condition and concrete strength. Since some of the specimens had debonding of the strands, a total of 184 zones were used in determining transfer lengths. Unlike some previous studies, this one consisted of 0.6-inch-diameter prestressing strand. Strand surface condition was a major component of this study, so for half of the specimens, the strand used had a bright surface condition and the other half were prestressed with rusted strand. Strand surface condition did not play a major role in increased transfer lengths over time. A mechanical strain gage was used to determine surface strains along both sides of the specimens and from this data, transfer lengths were obtained. It was found that transfer lengths increase approximately 10 to 20% over time. Almost all the increase occurred within the first 28 days after release. Average transfer length of the rusted strands was shorter than those of bright strands. However, it was found that the transfer lengths of rusted strands did see a much greater scatter in data than that of the bright strands.

The method of prestress release did not affect transfer lengths of the bright strands; however, a sudden release with the rusted strand did see a 30 to 50% increase in transfer length. The authors concluded that the expression

$$L_t = 0.17 \text{ ksi}^{-0.5} \left(f_{pt} / \sqrt{f_{ci}} \right) d_b \quad (2.16)$$

provides a lower bound for long-term transfer lengths measured in this study.

Khayat et al. (2003) studied bond strength of prestressing strands in wall elements. The strands were placed in the horizontal position and at different heights, and the pullout tests were performed on the strand. Four SCC and two conventional concrete mixtures were used for this study. Different types of curing methods were used on the concrete wall. The following conclusions were made:

- A top-bar effect did exist; however, it was different depending on the method of curing. The top-bar effect was greater for those mixtures cured by steam.
- Overall, the strand bond was not comprised in a stable SCC mixture.
- The top-bar effect is shown to be sensitive to the type of VMA used.
- For all mixtures, the top-bar effect in air-cured concrete was lower than steam-cured concrete.

Girgis and Tuan (2005) performed Moustafa pullout tests with SCC to determine bond strength. In addition, the transfer length of three pretensioned concrete bridge girders was measured. Three concrete mixtures were used in this study, two SCC and one conventional. The authors found that maximum pullout value was larger for the SCC mixture than the conventional concrete mixture. However, transfer lengths were greater for the girders utilizing SCC. It was concluded that

- Use of a viscosity-modifying admixture may adversely affect early compressive strengths and bond strength of the SCC, which will lead to greater transfer lengths;
- SCC mixtures experience higher transfer lengths than mixtures with conventional concrete;
- Moustafa pullout tests failed to reveal any early-age bond-strength reduction when using SCC;
- SCC had higher bond strength at 28 days, which may warrant shorter development lengths for girders with SCC; and
- Both SCC and conventional concrete in the pullout tests, the smaller the deformed bar, the higher the bond strength.

Burgueno and Haq (2005) evaluated transfer and development lengths of prestressed girders using both SCC and conventional concrete mixtures. Transfer lengths were determined by strand draw-in and concrete surface strains, while development lengths were obtained through flexural tests. The authors found that the ACI expression for transfer length was conservative for both SCC and conventional concrete mixtures. However, development lengths for the SCC mixtures were slightly larger than that predicted by code equations.

The 2005 “European Guidelines for Self-Compacting Concrete” state that no special provisions should be used for transfer and development length when using SCC. Studies have shown that the transfer length for strands embedded in SCC were on the safe side when compared with calculated values according to their current code

equations. Plus, a “top-strand” effect was not seen in members with SCC due to the fact that SCCs fluidity and cohesion minimize the negative effect of bleed water.

2.4 Current Development and Transfer Length Equations

Tabatabai and Dickson (1993) conducted a research study to determine the history behind strand development and transfer length equations. It was found that the current transfer length (equation 2.1) dates back to 1963 and was derived using data from the Portland Cement Association. It states that three factors affect bond; adhesion between concrete and steel, friction between concrete and steel and mechanical resistance between concrete and steel. An average transfer bond stress of 400 psi was used in determining the equation, but it is not clear as to where that number originated. The current equation for development length (equation 2.2) was first introduced in the 1963 ACI Building Code. The equation was based on published reports by Hanson and Kaar (1959) along with the work of Kaar et al(1963). However, those two reports do not propose equations for development length. It was also determined that Alan H. Mattock, who worked for the Portland Cement Association, was involved with proposing the current equations for both transfer and development length.

2.5 Bridge Monitoring

Detailed below are a few other projects that used vibrating-wire strain gages to monitor long-term strains in prestressed bridge girders. It must be noted that all of the projects used high-performance concrete, not SCC. At the time of this study, no literature on the monitoring of bridge girders with SCC could be found.

Ahlborn et al. (2000) investigated long-term prestress losses of two long-span, high-strength composite prestressed bridge girders in the state of Minnesota. They also determined the adequacy of AASHTO provisions for design. Vibrating-wire strain gages were embedded into the concrete to account for losses after the time of strand release. The authors believed the gages could not account for losses in the prestressing strand before the concrete hardened. They calculated total prestress losses from flexural cracking and crack-reopening loads. Losses that occurred before release were then back-calculated by taking total prestress losses and subtracting losses after release. The authors concluded the AASHTO design method overestimated the concrete modulus, leading to lower initial losses. Plus, the AASHTO design equations overpredicted creep and shrinkage losses, thus leading to higher long-term losses. They recommended great caution be used when using AASHTO design guidelines with high-strength concrete.

Barr et al. (2000) presented results of using high-performance concrete in prestressed, precast concrete bridge girders in the state of Washington. Vibrating wire-strain gages were embedded into the girders to measure temperature and long-term strains. From this data, a comparison with current design equations could be made. The authors concluded that by using high-performance concrete, engineers could reduce the number of girder lines used in a bridge. They also found that prestress losses were higher with girders using high-performance concrete than those girders using conventional concrete.

Ramakrishnan and Sigl (2001) instrumented two, three-span high-performance concrete bridges in the state of South Dakota. For the project, trial concrete mixes were

first tested and the mixture that resulted in the best performance was used in the bridge girders. The girders that were instrumented had vibrating wire transducers embedded into them. It was found that prestress losses were slightly larger than those predicted by code equations. The authors also recommend the concrete mixture be used for all state girders utilizing high-performance concrete. Also, a change for the calculation for modulus of elasticity of the concrete was also recommended.

Onyemelukwe et al. (2003) embedded vibrating wire-strain gages into an actual prestressed bridge in the state of Florida to examine time-dependent losses. They discuss the monitoring process and techniques used throughout their study. The authors compared experimental data with code estimates of PCI and AASHTO. It was determined that code estimates gave very close predications to actual experimental data. They also concluded that the methods used to instrument the bridge were very satisfactory.

Yang and Myers (2005) reported prestress losses observed for the first two years of the first high-performance superstructure concrete bridge in the state of Missouri. The authors compared the recorded losses to eight commonly used models for predicting prestress losses. Standard AASHTO Type-II girders were instrumented with vibrating wire-strain gages to obtain long-term losses. In all, 20 girders were used for the bridge, with four of those being instrumented. It was found that the girders behaved as expected and code equations used to predict prestress losses were fairly accurate.

CHAPTER THREE - DESIGN OF FLEXURAL SPECIMENS

Three separate cross sections were tested to evaluate current development length equations. The single strand specimens had identical cross sectional properties at the critical section tested in flexure (mid-span); however, at the specimen ends the cross sections were different in order to test the “top-strand” effect. Table 3.1 summarizes the three different specimens tested. More detail for each specimen type is given below.

Table 3.2: Properties of different cross sections

Specimen	Overall Height* (inch)	Depth to Strand* (inch)	Number of Strands
SSB	12	10	1
TSB	24	2	1
TB	21	19	5

* dimension at specimen end, not critical section at mid-span

3.1 Single-Strand Development Length Specimens

Twelve single-strand, development length specimens with two different embedment lengths were fabricated and tested. However, due to a handling error with one of the specimens, only 11 were tested to failure. In addition, these specimens utilized two different cross sections in order to evaluate the so-called “top-strand” effect, where 12 inches or more of concrete is cast below the strand. ACI requires a 1.3 multiplier on development length on deformed bars for “horizontal reinforcement so placed that more than 12 in. of fresh concrete is cast in the member below the development length or splice.” AASHTO uses a similar 1.3 multiplier for strand

development length when using an alternate development length equation in section 5.11.4.2.

The first cross section cast was an 8-inch \times 12-inch rectangular section. The nomenclature used for these specimens was single-strand beams (SSB). The section contained a single prestressing strand at a depth d_p of 10 inches (Figure 3.1). This section was chosen slightly larger than the 6.5-inch wide specimen tested by Logan in order to provide increased shear capacity. This was desirable because these specimens did not have any shear reinforcement (see A.3 for shear-capacity calculations). The strain in the strand at nominal flexural capacity (see A.4 for sample calculations) was estimated to be 2.94%, using strain compatibility analysis. This value is lower than the 3.5% recommended by Buckner for minimum strand strains in development length specimens. However, it is larger than the 2.0% value calculated by Logan for single-strand beams tested in his investigation and failed in flexure by strand rupture.

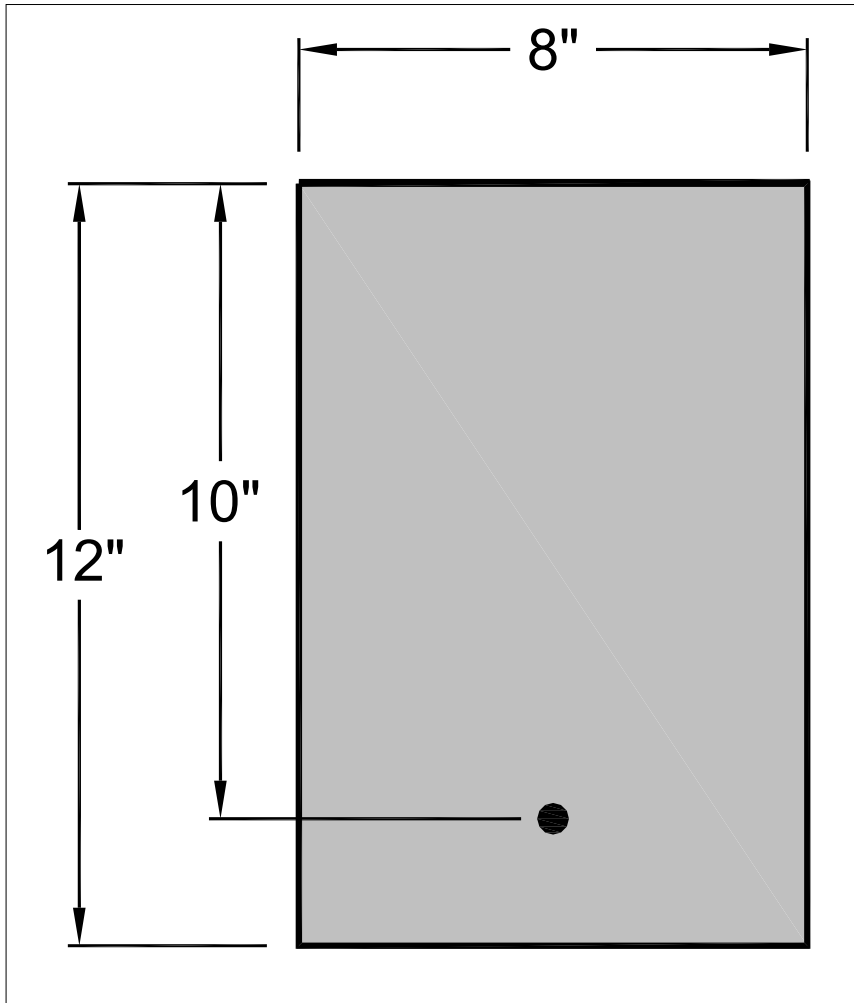


Figure 3.1: Cross section of bottom-strand specimens

Specimens used to evaluate the “top-strand” effect, are denoted top-strand beams (TSB). These specimens had a width of 8 inches and an overall height of 24 inches (Figure 3.2). The strand in these specimens was located 22 inches from the bottom, and thus greatly exceeded the 12-inch height requiring a 1.3 multiplier for development length by AASHTO. However, at mid span, a Styrofoam® block-out was used to reduce the height from 24 inches to 12 inches, as shown in Figure 3.3. These specimens were inverted prior to testing. Note that at mid span, which is the critical section, these

specimens had identical cross sections to the SSB specimens. Therefore, direct comparison between results is justified.

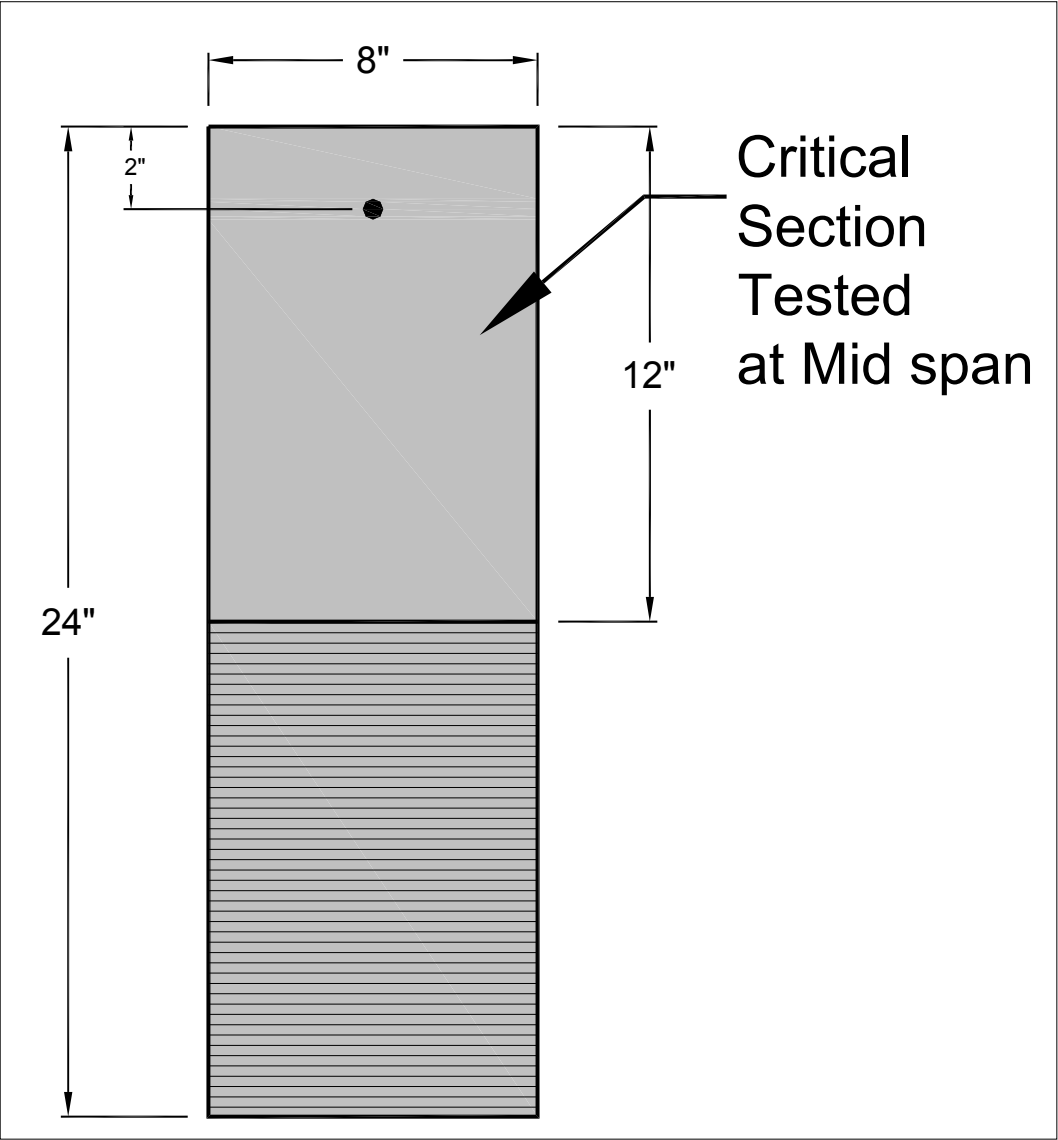


Figure 3.2: Cross section of top-strand specimens



Figure 3.3: Block-out used for top-strand beams

3.2 Multiple-Strand Development Length Specimens

In addition to the single-strand specimens, four multiple-strand specimens were cast in order to investigate the development length of multiple strands at close spacing. These specimens had a T-shape in order to provide the necessary compression area to produce high-tensile strains in the strand at nominal-moment capacity. The calculated strain in the strand was larger than 3.5%, based on strain compatibility (see A.5 for nominal-moment calculation). The nomenclature used for these **I**-beams was simply TB. The cross section of these specimens was identical to the ones used by Peterman et al. in their test program. The cross section had five bottom 0.5-inch-diameter strands at a depth of 19 inches and an overall height of 21 inches, and a compression flange width of 36 inches (Figure 3.4). Half-inch-diameter rebar stirrups at 6 inches on center were used in both the web and flange, which satisfied ACI code provisions for shear (Figure 3.5). (ACI 318, 2002)

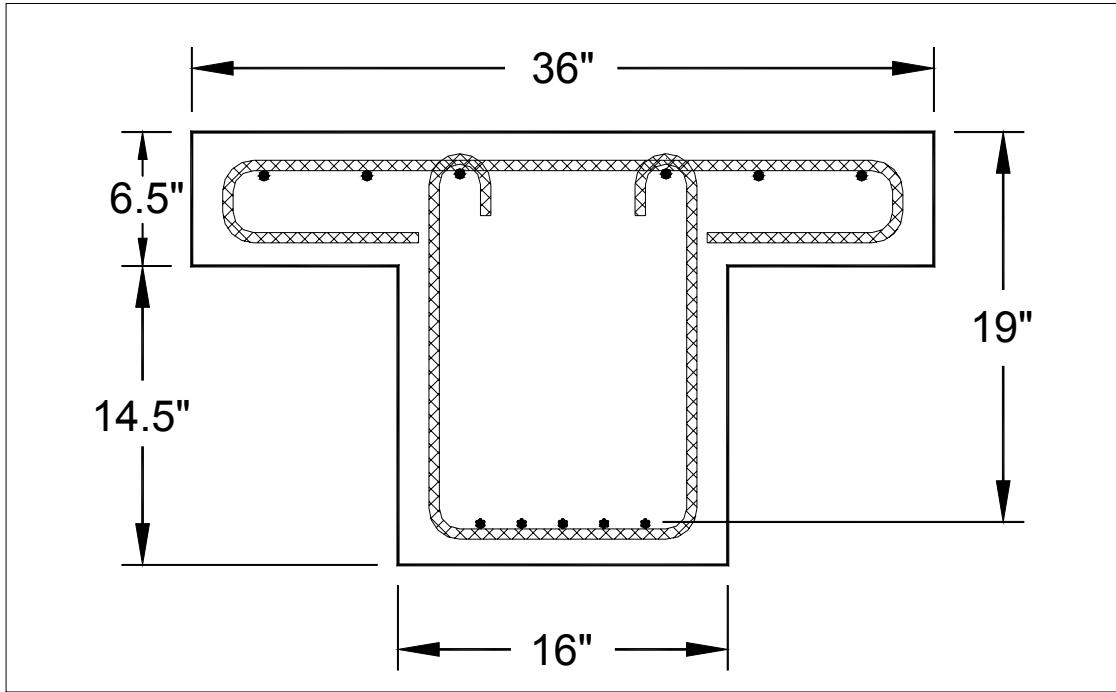


Figure 3.4: Cross section of T- beam specimen



Figure 3.5: Shear reinforcement for T-beams

3.3 Embedment Lengths

At the outset of this experimental program, it was determined that two different embedment lengths, l_e , were to be tested. Crack formers, as in Figure 3.6 for the SSB specimens, Figure 3.7 for the TSB specimens, and Figure 3.8 for the TB specimens, were cast at the embedment length to ensure that during loading the first cracks would open at these locations.



Figure 3.6: Crack former in SSB specimens



Figure 3.7: Crack former for TSB specimen



Figure 3.8: Crack former used for TB specimens

The first set of specimens were tested at an embedment length equal to 100% (6'-1") of the calculated development length, l_{dev} , as shown in Figure 3.9 for SSB setup (and very similar for the TB setup) and Figure 3.10 for TSB setup. The second set of specimens were tested at either 80% l_{dev} or 120% l_{dev} , depending on results obtained from the 100% l_{dev} specimen tests. The second set of specimens were specifically designed to allow for testing at either embedment length as explained in the following.

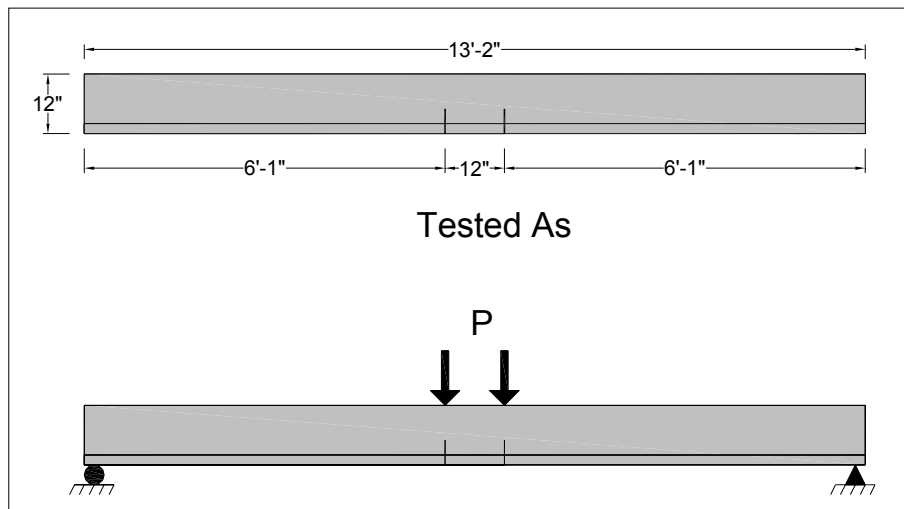


Figure 3.9: Test setup for 6'-1" embedment length (SSB and TB)

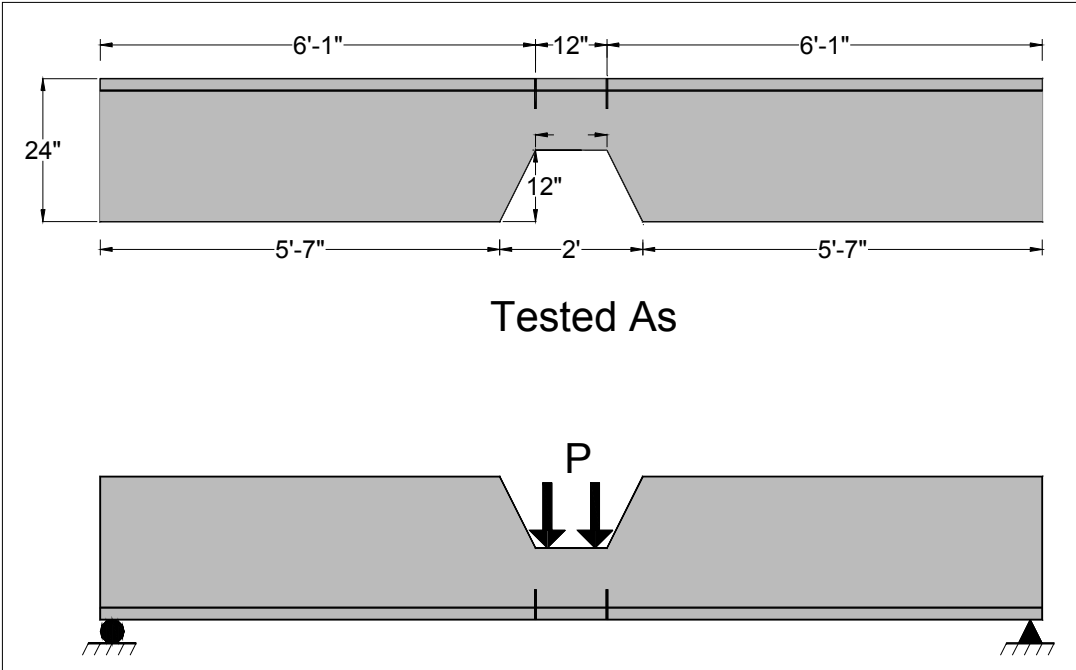


Figure 3.10: Test setup for 6'-1" embedment length for TSB specimens

If the 100% l_{dev} specimens failed (by flexure) at a moment greater than or equal to the calculated nominal-moment capacity M_n , then the second set of specimens would be tested at an embedment length equal to 80% l_{dev} (4'-10"). However, if the 100% l_{dev} specimens failed (by bond) at a moment less than the calculated nominal-moment capacity M_n , then the second set of specimens would be tested at an embedment length equal to 120% l_{dev} (7'-3"). Because all of the 100% l_{dev} specimens failed by flexure (as will be discussed in the Chapter Seven of this manuscript), the second set of specimens were all tested at an embedment length equal to 80% l_{dev} . TSB setup is shown in Figure 3.11.

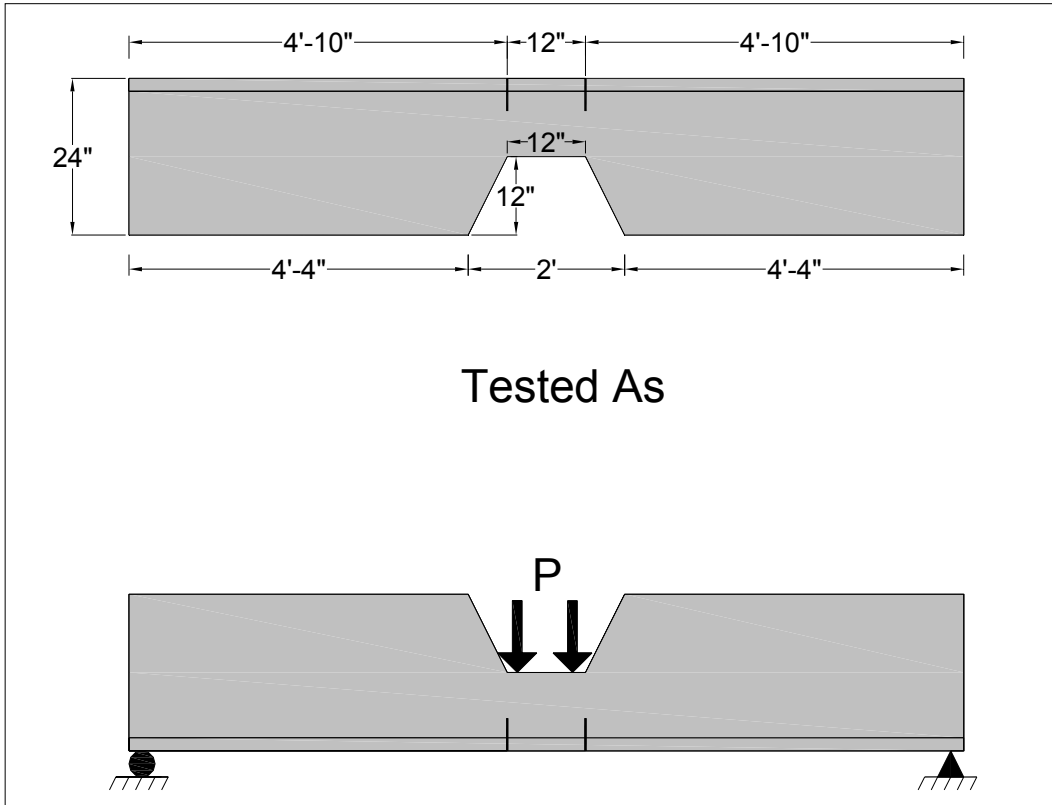


Figure 3.11: Test setup for 4'-10" embedment length TSB specimens

The different embedment length testing of the second set of specimens was made possible by utilizing four crack formers per beam (Figure 3.12). As shown in this figure, the 80% I_{dev} tests required use of the spreader beam with loading points directly above the outer-most crack former, as shown in Figures 6.34 and 6.35.

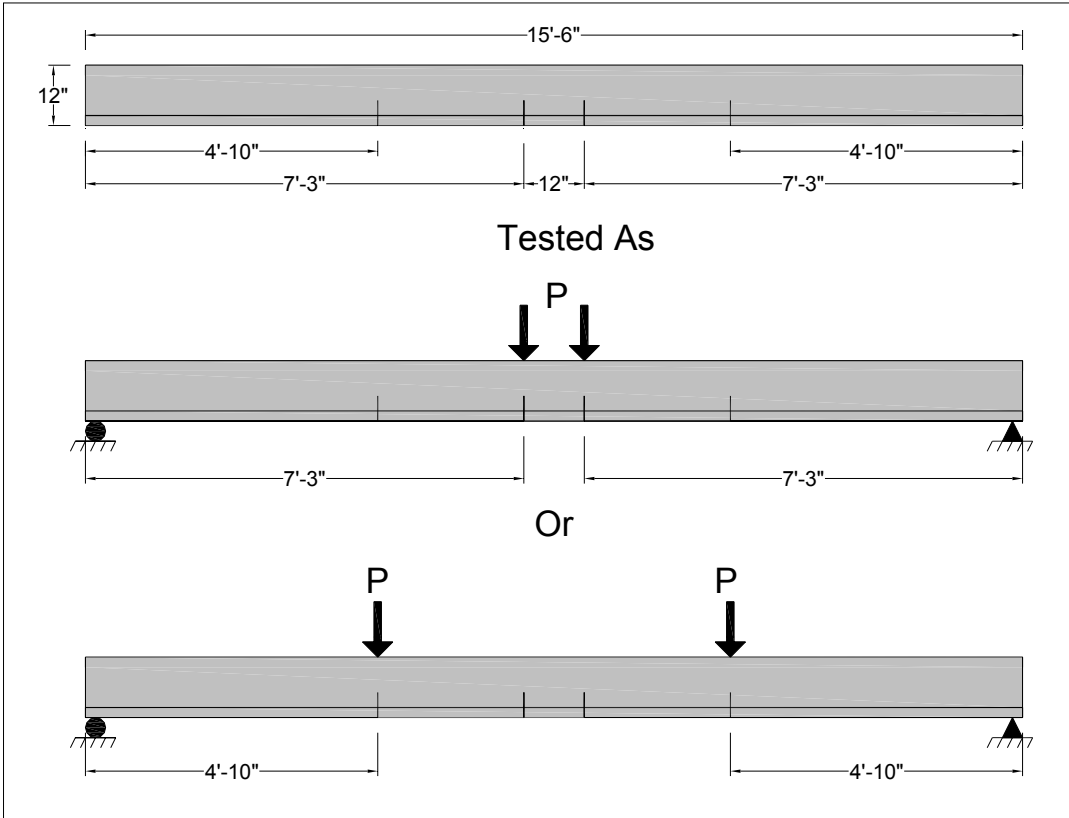


Figure 3.12: Test setup for 4'-10" embedment length SSB and TB specimens

CHAPTER FOUR - MATERIAL PROPERTIES

4.1 Large-Block Pullout Tests

Prior to casting any flexural test specimens, the prestressing strand that would be used for all test girder specimens was pre-qualified using the LBPT procedure, Figure 4.1. Standard LBPT procedures, as stipulated by Logan, were followed in these tests. These strand qualification tests were performed with the standard mix proposed by Logan (Table A.1) and not with SCC. Results of these tests are shown in Table 4.1. The compressive strength of the Logan mixture was 5,600 psi. The average first-observed slip was at 21.6 kip, and the average ultimate pullout was 39.6 kip. The values are both above the minimum recommended values of 16 kip and 36 kip, respectively, and meet the maximum coefficient of variation of 10% for a six-sample group. Thus, the strand reel was deemed acceptable for use in this study. This reel was then covered to prevent weathering and used for all flexural beam tests and IT specimens reported herein.



Figure 4.1: LBPT setup

Table 4.1:: LBPT with Logan concrete and project strand

Logan Concrete with Project Strand		
Specimen	Max Load (kip)	Load at 1st Slip (kip)
1	41.3	21.9
2	41.4	20.8
3	41.5	23.4
4	40.5	19.4
5	35.8	20.2
6	37.1	23.8
Average	39.6	21.6
Coeff. of Var.	6.3%	8.1%

4.2 Mix Design

Casting of test specimens was performed at Prestressed Concrete Inc., Newton, Kansas, which is a PCI-certified plant that produces bridge members. They developed their proposed SCC mixture design with the help of their admixture supplier. The SCC mixture used in this study, along with the conventional concrete mixture that this plant uses, is presented in Table 4.2. This conventional concrete mixture is used in some of the girders for the Cowley County Bridge, as described in Chapters 12 and 13. It should be noted that both mixes use a ¾-inch maximum aggregate size and have a 0.30 and 0.41 water-to-cementitious materials ratio for the SCC and the conventional concrete mixtures, respectively. Also note that a different high-range water reducer is used for the SCC and conventional concrete mixtures.

Table 4.2: SCC and conventional concrete mixture proportions

	SCC	Conventional
Materials	Quantity per yd³	Quantity per yd³
Cement (Type III)	750 lbs	650 lbs
Fine Aggregate	1500 lbs	1480 lbs
Coarse Aggregate	1360 lbs	1457 lbs
Air Entrainment	5 oz	6 oz
HRWR	70 oz	26 oz
VMA	0 oz	0 oz
Water	27 gal	31.6 gal
w/c ratio	0.30	0.41

4.3 Fresh Concrete Evaluation

During casting of the specimens, the SCC mixture was tested to determine its workability. At the time of casting, there were no existing ASTM standards for testing SCC, but the PCI Interim Guidelines documents have many test methods to evaluate the plastic properties of SCC for production qualifications. However, since the time of testing ASTM has adopted two standards for the evaluations of SCC. The two standards were ASTM C1611 “Standard Test Method for Slump Flow of Self-Consolidating” and ASTM C1621 “Standard Test Method for Passing Ability of Self-Consolidating Concrete by J-Ring.” In this study, inverted-slump flow and visual stability index (VSI) (Figure 4.2), J-Ring (Figure 4.3), and L-Box (Figure 4.4) tests were all performed on the concrete during casting. Khayat et al. outlined the procedures for performing these tests. The inverted-slump flow (spread) measures SCC consistency. It also evaluates the capability of concrete to deform under its own weight. The J-Ring and L-Box are used to evaluate passing ability and blocking resistance of the SCC mix. Khayat et al. reported the difference between the inverted-slump flow (spread) and J-

Ring should not exceed two inches. A schematic of the L-Box is located in the “Interim Guidelines for the Use of Self-Consolidating Concrete in PCI Member Plants”. Khayat et al. reported that an 0.80 to 1.0 ratio for h_2/h_1 for L-Box tests has been proposed, but has not been passed into ASTM standard test methods.



Figure 4.2 Inverted slump for SCC



Figure 4.3: Ring test for SCC



Figure 4.4: L-Box test for SCC

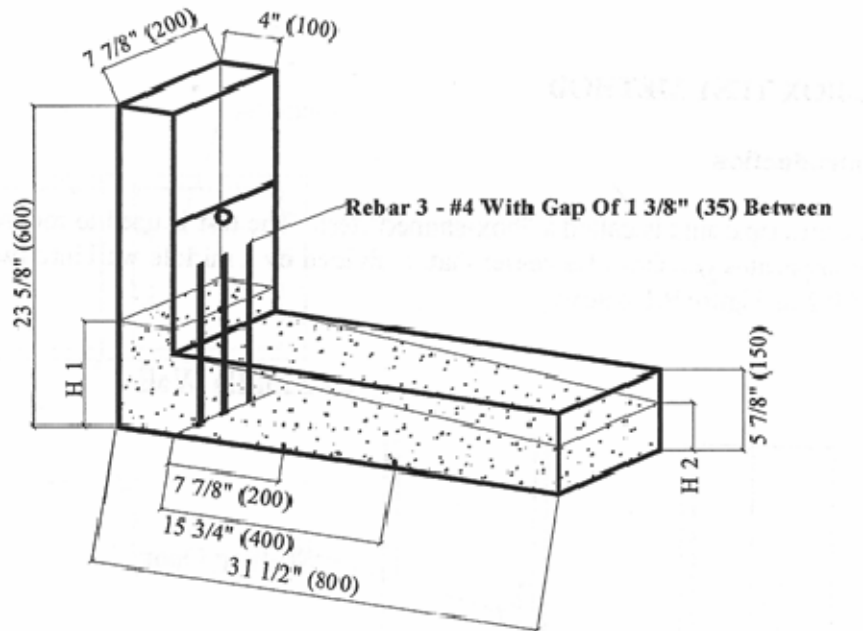


Figure 4.5: Schematic of L-Box (Interim Guidelines, 2003)

4.4 Hardened Concrete Properties

The compressive strength and modulus of elasticity of the concrete were measured for future use in analytical computations. Standard ASTM procedures were followed for compressive strength and modulus of elasticity testing. In addition to measuring one-day (release) compressive strengths, compressive strengths were determined just prior to loading the flexural specimens to failure. A set of three, 4-inch x 8-inch cylinders were tested for each flexural specimen, and average values were determined. A typical compressive strength versus time curve for the proposed SCC mixture is shown in Figure 4.6.

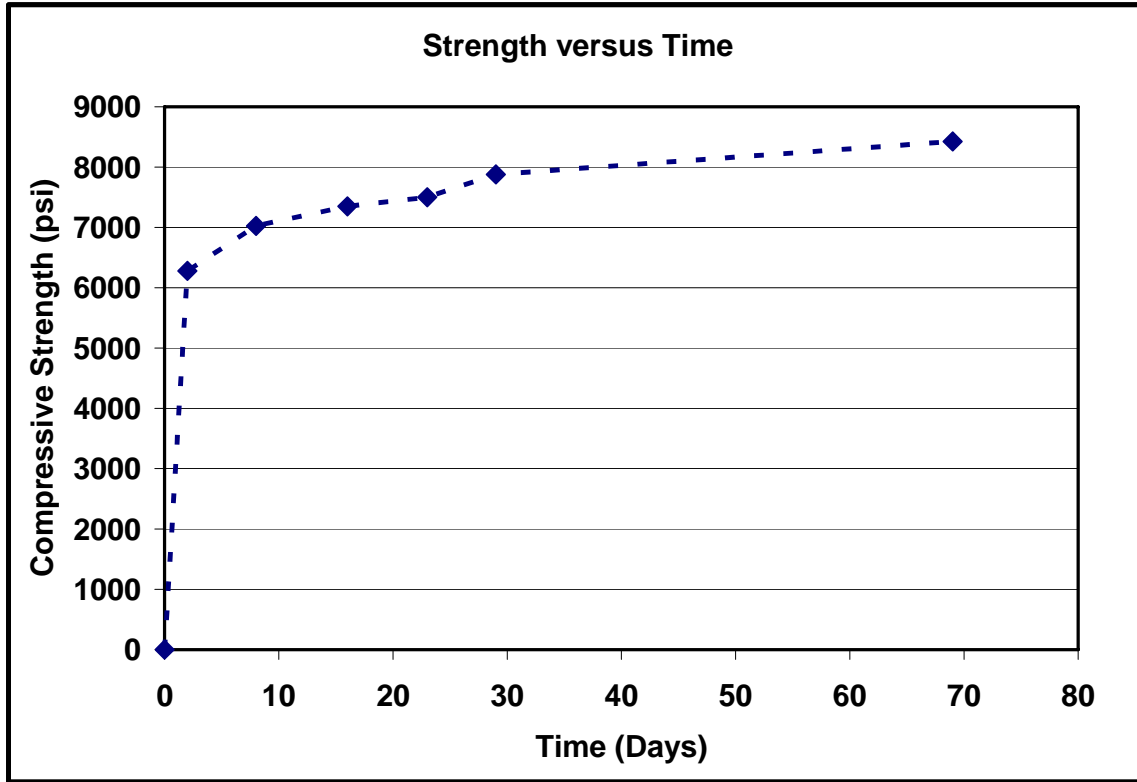


Figure 4.6: Compressive strength development for SCC

CHAPTER FIVE - DETERMINATION OF TRANSFER LENGTH

5.1 End Slip Measurements

End-slip measurements were used in determining transfer lengths of each end for the flexural specimens. End slip can also be described as the amount that the strand “draws” into the specimen end. Transfer length is a key parameter for shear design of prestressed concrete members. If the actual transfer length of the member is larger than the assumed value of 50 strand diameters (governed by ACI), then a possible shear deficiency may occur in the member. For this reason, it is important that transfer length of a member be accurately determined.

Measuring the amount of end slip that the strand undergoes has proven to be an effective way of determining transfer lengths. Russell and Burns (1996) state that “a statistical correlation does exist between transfer length and strand end slips,” and suggest that end slips may reliably predict transfer lengths. Logan (1997) also measured strand end slip and found it to be a very accurate measure of transfer length.

Mast’s strand-slip theory as presented by Logan (1997) was used to determine transfer length of the girders experimentally. Many publications have shown that a theoretical relationship exists that relates transfer length as a function of strand slip. The equation was derived by assuming a straight-line variation in strand stress from zero at the end of the beam to full prestress at the transfer length (Logan 1997). The end slip can then be expressed in terms of the reduction of the stress in the strand due to release of the prestressing strand. The following equation can be used to determine the implied transfer length of a member.

$$L_{tr} = \frac{2E_{ps}\Delta}{f_{si}} \quad (5.1)$$

where

E_{ps} = modulus of elasticity of the prestressing strand (ksi);

Δ = amount of strand slip (inches); and

f_{si} = stress in prestressing strand immediately after transfer of prestress force to concrete (ksi).

Different methods have been used to measure the amount of strand slip the strand undergoes. The following method outlines the procedure that was used in this study:

- Prior to detensioning, a mark was made on the strand with a saw blade at a distance approximately 1 inch from the specimen end, Figure 5.1.
- After detensioning, the elastic shortening that occurred in this one inch distance was subtracted from the total amount of end slip, as seen in the following sample calculation,
- A steel block having an exact width of 0.500 inches was held against the concrete at the strand location.
- The distance between this machined block and the mark on the strand was then measured using a digital caliper having a precision of 0.001 inch, Figure 5.2.
- This value was used as the baseline for measurements taken after detensioning to determine the amount of end slip.
- Subsequent end-slip measurements were taken up to the time of testing for each specimen.



Figure 5.1: Making notch on prestressing strand



Figure 5.2: Measuring distance between notch and steel block

The following sample calculation, for the single-strand specimens, detail the equations used in determining the implied transfer length values from the end-slip measurement data.

Measured distance before detensioning = 0.524 inches

Measured distance after detensioning = 0.463 inches

Raw end slip = 0.524 inch - 0.463 inch = 0.061 inches

$$\text{Elastic shortening of strand} = \frac{PL}{A_{ps}E_{ps}} = \frac{31(1)}{0.153(28,500)} = 0.0071$$

where

P = force in strand, kips;

L = length of strand between notch and specimen end, inch;

A_{ps} = area of prestressing strand, inch²; and

E_{ps} = modulus of elasticity of prestressing strand, ksi.

End slip = Δ = raw end slip – elastic shortening of strand

Δ = 0.061 inch – 0.0071 inch = 0.054 inches

$$L_{tr} = \frac{2E_{ps}\Delta}{f_{si}} = \frac{2(28,500)0.054}{196} = 16 \text{ inches}$$

with the calculation of f_{si} shown in A.6.

5.2 Surface Strain Measurements

Concrete surface strains were used in determination of the transfer length for the IT specimens. A mechanical strain gage (Whittemore gage, Figure 5.3) was used to measure the surface strains. Whittemore points, stainless steel discs with a machined hole in the center, were adhered along the bottom flange of the specimen prior to detensioning, Figure 5.4. Readings were taken just prior to detensioning and after detensioning. Then the concrete strain at transfer was determined by taking the numerical difference between the initial reading and the final reading. The measured concrete strains were then plotted against the length of the specimen. To reduce any anomalies, measured strains were smoothed by averaging the data over three gage lengths. The equation used to smooth the data is shown as follows:

$$(\text{strain})_i = \frac{(\text{strain})_{i-1} + (\text{strain})_i + (\text{strain})_{i+1}}{3} \quad (5.2)$$

where

i = the current strain reading.

Hence, at any given strain point, strain and the values just ahead and behind were averaged to obtain the “smoothed” curve.

Transfer lengths for each specimen end were then determined by plotting the concrete strains versus the specimen length and evaluating the strain profile. Russell and Burns (1993)² developed a simple procedure for determining transfer lengths from the strain profiles. The procedure is known as the “95% average maximum strain” and is outlined below.

- Plot the “smoothed”-strain profile by taking the average of three consecutive strain points.
- Determine the “average maximum strain” by computing the average of all strains contained within the strain plateau of the fully effective prestress force.
- Take 95% of the above calculated “average maximum strain” and construct a line corresponding to this value.
- Transfer length is determined by taking the intersection of the 95% maximum strain line and the “smoothed”-strain profile line.



Figure 5.3: Whittemore gage



Figure 5.4: Whittmore locating points

CHAPTER SIX - FABRICATION AND TEST SETUP OF FLEXURAL SPECIMENS

6.1 Flexural Specimen Fabrication

Fabrication of all flexural specimens was performed at Prestressed Concrete Inc., Newton, Kansas. All six bottom strand beams along with TB A and TB C were cast in the afternoon of March 29, 2004, and detensioned the next morning, March 30, 2004. The remaining two T-beams, TB B and TB D, were cast in the afternoon of March 30, 2004, and detensioned the next morning, March 31, 2004. On the afternoon of April 8, 2004, nine top-strand beams were cast and detensioned the next morning, April 9, 2004. Table 6.1 presents a review of the cast date and detensioning date for each specimen.

Table 6.1: Review of cast and detensioning dates

	Beam	Date Cast	Date of Detensioning
Bottom Strand	SSB A	3/29/2004	3/30/2004
	SSB C	3/29/2004	3/30/2004
	SSB D	3/29/2004	3/30/2004
	SSB E	3/29/2004	3/30/2004
	SSB F	3/29/2004	3/30/2004
Top Strand	TSB A	4/8/2004	4/9/2004
	TSB B	4/8/2004	4/9/2004
	TSB C	4/8/2004	4/9/2004
	TSB D	4/8/2004	4/9/2004
	TSB E	4/8/2004	4/9/2004
	TSB F	4/8/2004	4/9/2004
T-Beams	TB A	3/29/2004	3/30/2004
	TB B	3/30/2004	3/31/2004
	TB C	3/29/2004	3/30/2004
	TB D	3/30/2004	3/31/2004

Two vibrating wire strain gages (VWSG) were embedded in three of the specimens (SSB A, TSB D, and TB A) to monitor long-term strains before testing. For SSB A, one gage was placed at strand height, two inches from the bottom and the other at 8.5 inches from the bottom, Figure 6.1. TSB D had one gage at strand height two inches from the bottom once the specimen was flipped, and the other at 8.5 inches from the bottom after the specimen was flipped, Figure 6.2. For TB A, one gage was located at strand height two inches from the bottom and the other at 19 inches from the bottom, Figure 6.3. To record the temperatures while the SCC was curing, digital temperature data loggers, Figure 6.4, were also placed in those three specimens to develop a temperature versus time curve.



Figure 6.1: VWSGs for SSB A



Figure 6.2: VWSG for TSB D

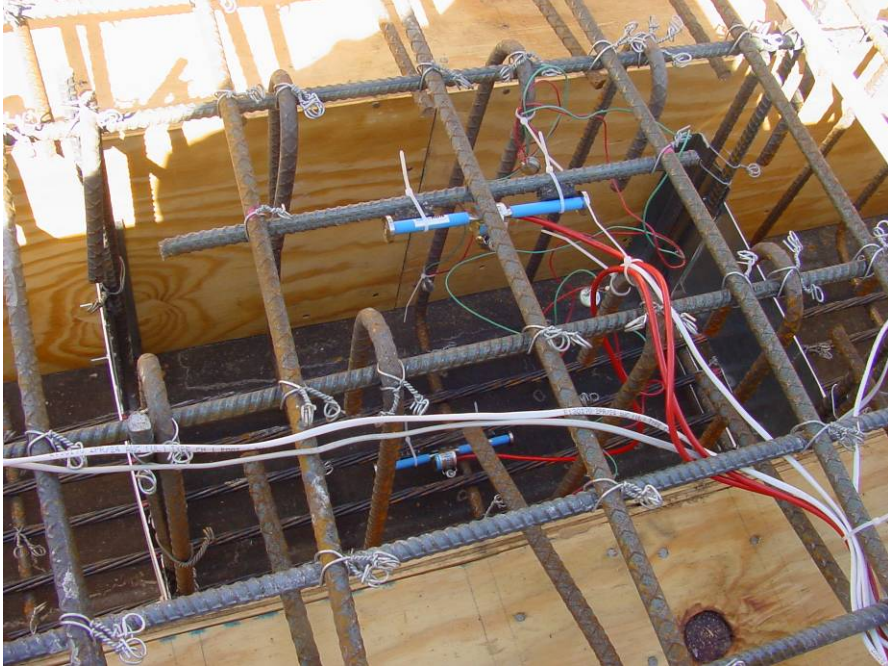


Figure 6.3: VWSGs for TBA

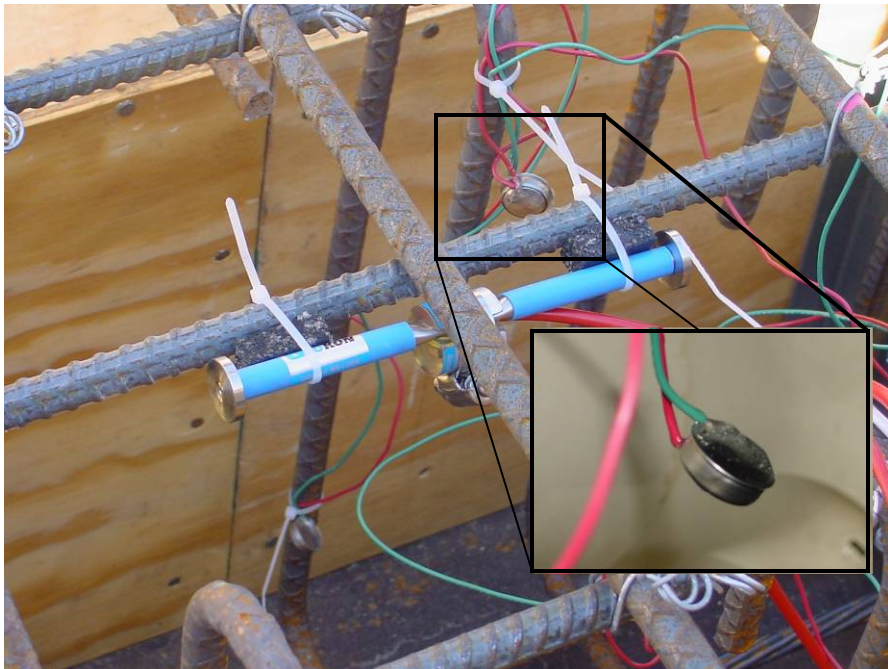


Figure 6.4: Digital temperature data logger to record temperature

Casting of the SSB specimens was a relatively short process. Forms with the dimensions of one foot wide by one foot deep were used to cast these specimens and Styrofoam sheets were used to get the correct width of the beams, Figure 6.5. The crack formers were held in place with use of wood across the top because no internal shear stirrups were used in these test specimens, as shown in Figure 6.6.



Figure 6.5: SSB bed



Figure 6.6: Crack former held in with wood 2 x 4

Once the forms were set to the correct dimensions and all test equipment was put in place, the SCC was poured into them, Figure 6.7, and then finished with a float, Figure 6.8. After release strength was met, Figure 6.9, the strand was torched and the specimens removed from the beds and moved to the field. They were then shipped up to Manhattan, Kansas, for testing.



Figure 6.7: Pouring of SCC into forms



Figure 6.8: Finishing of SSB specimens



Figure 6.9: Cured SSB

The TSB specimens utilized the rollaway bed for their casting, Figure 6.10. The walls were spaced at eight inches to accomplish this task. As noted earlier, a Styrofoam block was used to reduce the height at mid-span from 24 inches to 12 inches, Figure 6.11. Two, 0.75-inch-diameter rebar, which can be seen in Figures 6.10 and 6.11, was placed at the bottom of the beams to reduce the risk of cracking while the

specimens were flipped over. The Styrofoam blocks were removed and rebar cut prior to testing.



Figure 6.10: TSB bed with headers in place



Figure 6.11: Block used to reduce height at mid span

Coil inserts, Figure 6.12, were cast in the ends of each TSB specimen because no lift loops could be cast into the top of the specimens. These would later be used to remove the specimens from the bed and flip them over.



Figure 6.12 Inserts cast into ends so specimens could be flipped over

After the forms were set to the proper dimensions, the SCC was poured into the forms, Figure 6.13, and then finished, Figure 6.14.



Figure 6.13: Pouring of SCC into forms



Figure 6.14: Finishing of specimens

After the specimens had cured and release strength had been met, they were detensioned and the walls were removed, Figure 6.15. Once they had cured to the specified shipping strength, they were shipped to Manhattan, Kansas, for testing.



Figure 6.15: Removal of TSB from beds

The TB specimens were also cast on the rollaway bed, two at a time. The beds were first prepped and the headers were spaced at the proper distance, Figure 6.17. The web stirrups were placed and the strand was then pulled into place. The web and flange stirrups were tied into place, Figures 6.17 and 6.18.



Figure 6.16: Headers spaced for TB specimens



Figure 6.17: Placement of internal shear stirrups



Figure 6.18: Finished shear stirrups in TBs

Once the stirrups were all tied into place, the outside form walls were put in place, Figure, 6.19. The SCC was then poured into the forms, Figure 6.20, and finished using a float, Figure 6.21.



Figure 6.19: Placement of outside walls



Figure 6.20: Pouring of SCC into forms



Figure 6.21: Finishing of top surface

The next morning, after release strength was achieved, the strand was detensioned by flame cutting, Figure 6.22. Once the specimens had reached the proper strength, they were shipped to Manhattan, Kansas. As-built dimensions of each specimen can be seen in Table A.7.



Figure 6.22: Torching of strand of TBs

6.2 Flexural Specimen Setup

6.2.1 Test Setup

The flexural specimens were tested using MTS servo-controlled actuators in the KSU Civil Engineering Structural Mechanics Laboratory. The SSB and TSB specimens were moved into the testing laboratory by carts as shown in Figure 6.23. Larger carts had to be constructed to handle the larger TB specimens, Figure 6.24.



Figure 6.23: Carts used for SSB and TSB specimens



Figure 6.24: Carts for TB specimen

Data was collected for load, mid-span deflection, and strand end slip. End-slip readings were monitored using a linear variable differential transformer (LVDT), as shown in Figure 6.25 for the single-strand specimens and Figure 6.26 for the TB specimens.

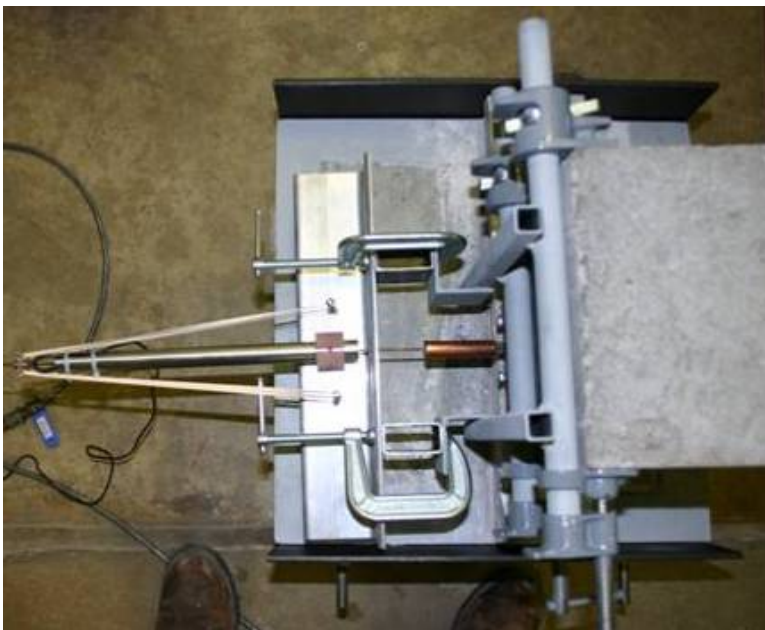


Figure 6.25: End-slip device used for SSB and TSB

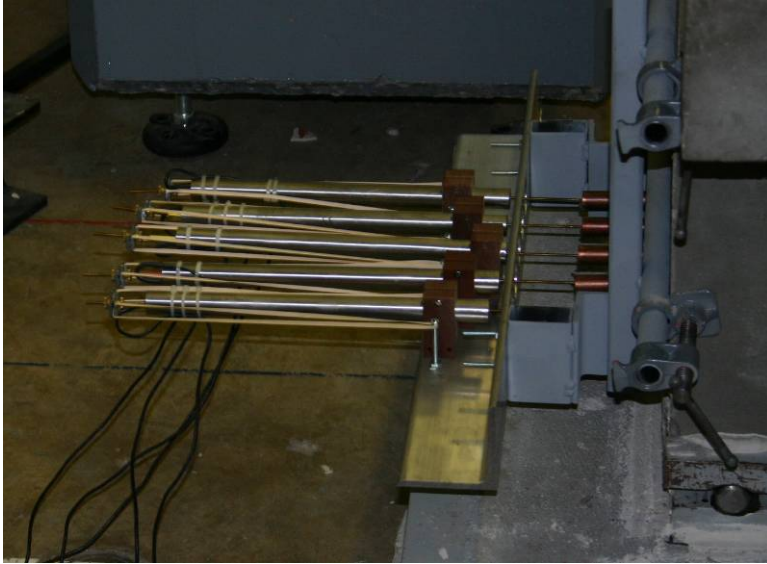


Figure 6.26: End-slip device used for TB specimens

LVDTs were also used to measure mid-span deflection. One on either side of the specimen was used, and the average value was used for data analysis, Figure 6.27.



Figure 6.27: LVDTs used for mid-span deflection

Figure 6.28 shows the test frame setup that was used to load all single-strand specimens. A spreader beam with rollers was used to apply point loads directly above the crack formers. Roller connections applied the point load at these locations. Figure

6.29 shows the TSB specimens in the loading frame. The TB specimens were loaded in the frame as shown in Figure 6.30.



Figure 6.28: Setup used for SSB specimens



Figure 6.29: Setup used for TSB specimens



Figure 6.30: Setup for TB specimens

The SSB and TB specimens, with 80% embedment lengths, had to utilize a spreader beam to apply the load. This was discussed in the embedment length section (section 3.3). The spreader beam used for the SSB specimens is shown in Figure 6.31 and Figure 6.32 for the TB specimens.



Figure 6.31: Spreader beam for SSB specimens



Figure 6.32: Spreader beam used for TB specimens

All specimens were taken to failure and are shown in Figures 6.33 to 6.35 for all three specimen types.



Figure 6.33: Failure for SSB specimen



Figure 6.34: Failure for TSB specimen



Figure 6.35: Failure for TB specimen

6.2.2 Loading Conditions

Three types of loading-rate conditions were used for evaluating the different embedment lengths. The first loading condition was designated as the SLOW test and was targeted to take about 10 hours. During a SLOW test, the specimen was loaded at 100 lb/min until cracking. Then the loading rate was reduced to 10 lb/min until failure. This slow loading rate was used to accurately measure the amount of strand slip, if any,

occurring prior to failure. For the second loading condition, designated as 76.5 % M_n , the specimen was loaded at 100 lb/min up to 76.5% of nominal capacity of the specimen and this load maintained for 24 hours. This load condition was modeled after ACI 318 section 20.3.2 for the testing and evaluation of existing structures. If the specimen successfully withstood the load for 24 hours, it was then loaded at 10 lb/min to failure. The final loading condition, designated as 100% M_n , was similar to the 76.5% M_n procedure, except that load was maintained at 100% M_n for 24 hours. Because only two types of the TB specimens were cast, the 76.5 % M_n and 100% M_n were combined for the second specimen to produce a more severe loading condition. Table 6.2 shows the loading condition of each specimen tested, along with the corresponding development length.

Table 6.2: Loading conditions for all specimens

	Beam	Embedment Length	Loading Condition
Bottom Strand	SSB A	6'-1"	76.5% M_n
	SSB C	6'-1"	SLOW
	SSB D	4'-10"	100% M_n
	SSB E	4'-10"	SLOW
	SSB F	4'-10"	76.5% M_n
Top Strand	TSB A	4'-10"	76.5% M_n
	TSB B	4'-10"	100% M_n
	TSB C	4'-10"	SLOW
	TSB D	6'-1"	100% M_n
	TSB E	6'-1"	76.5% M_n
	TSB F	6'-1"	SLOW
T-Beams	TB A	6'-1"	SLOW
	TB B	6'-1"	SLOW
	TB C	4'-10"	Combined
	TB D	4'-10"	Combined

CHAPTER SEVEN - FLEXURAL SPECIMEN RESULTS

7.1 Material Properties

Spread, VSI, J-Ring, and L-Box tests were performed before the casting of all flexural specimens. In addition, the compressive strength of concrete cylinders, that were matched-cured up to detensioning, were completed at the time of prestress release and just before the specimens were brought to failure. The ASTM C 39 standard for performing compressive strength tests was followed. Table 7.1 summarizes all of the measured concrete properties. The inverted-slump flow (spread), J-Ring, and L-Box tests were all performed before pouring of SCC into the forms. The VSI was determined by the author and the other tests were performed by the author and plant personal.

Table 7.1: Concrete properties of specimens tested

	Specimen	Slump Flow (inch)	VSI	J-Ring (in.)	L-Box (h_2/h_1)	Strength @ Release (psi)	Strength @ Testing (psi)
Bottom Strand	SSB A	21	0.5	19	0.80	5,000	8,250
	SSB C	21	0.5	19	0.80	5,000	6,960
	SSB D	22	0.5	21	0.83	5,000	7,430
	SSB E	22	0.5	21	0.83	5,000	7,710
	SSB F	22	0.5	21	0.83	5,000	7,190
Top Strand	TSB A	28	0.5	26 1/2	0.88	3,600	6,570
	TSB B	28	0.5	26 1/2	0.88	3,600	7,150
	TSB C	28	0.5	26 1/2	0.88	3,600	6,940
	TSB D	28	0.5	26 1/2	0.88	3,600	7,790
	TSB E	28	0.5	26 1/2	0.88	3,600	7,330
	TSB F	28	0.5	26 1/2	0.88	3,600	6,100
T-Beams	TB A	17	0.5	14	0.78	5,200	7,550
	TB B	22	0.5	21	0.83	4,800	7,920
	TB C	21	1.0	18 1/2	0.83	5,200	8,300
	TB D	22	0.5	21	0.83	4,800	8,070

The temperature of the SCC was recorded during curing for three of the flexural specimens and a typical heat development curve for 24 hours is shown, Figure 7.1, Figure 7.2, and Figure 7.3 for the SSB, TSB, and TB specimens, respectively. It must be noted that the TSB and TB specimens had greater mass and thus were able to generate more heat during curing.

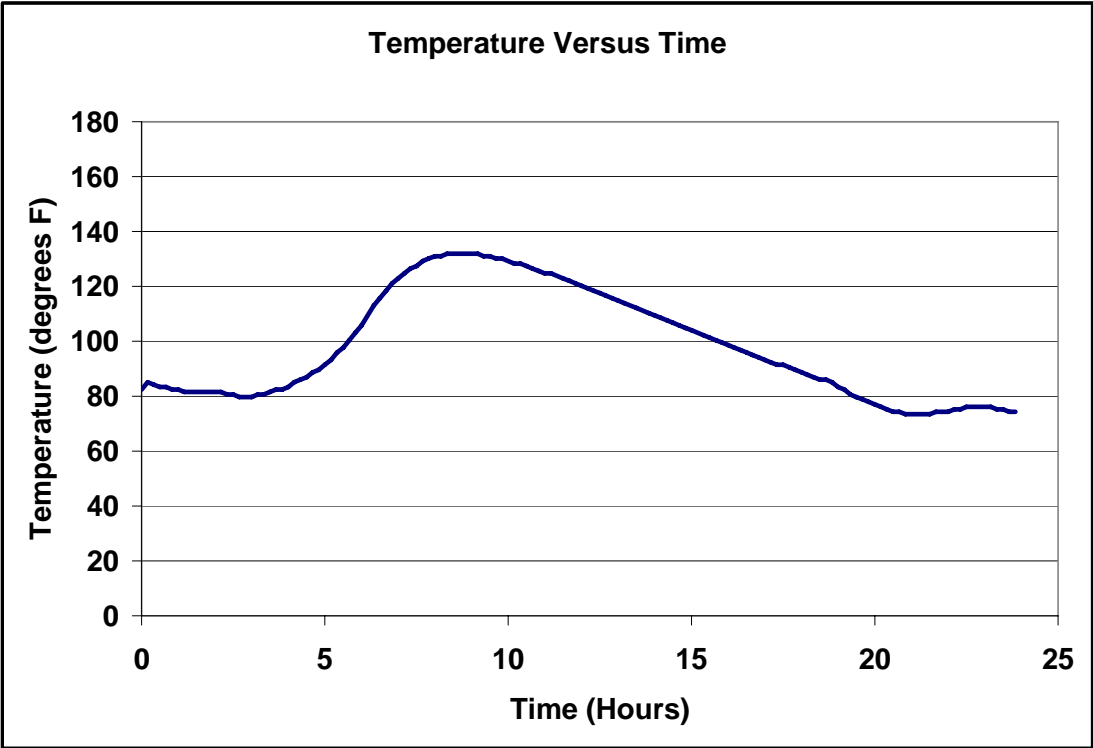


Figure 7.1: Temperature curve during curing for SSB specimen

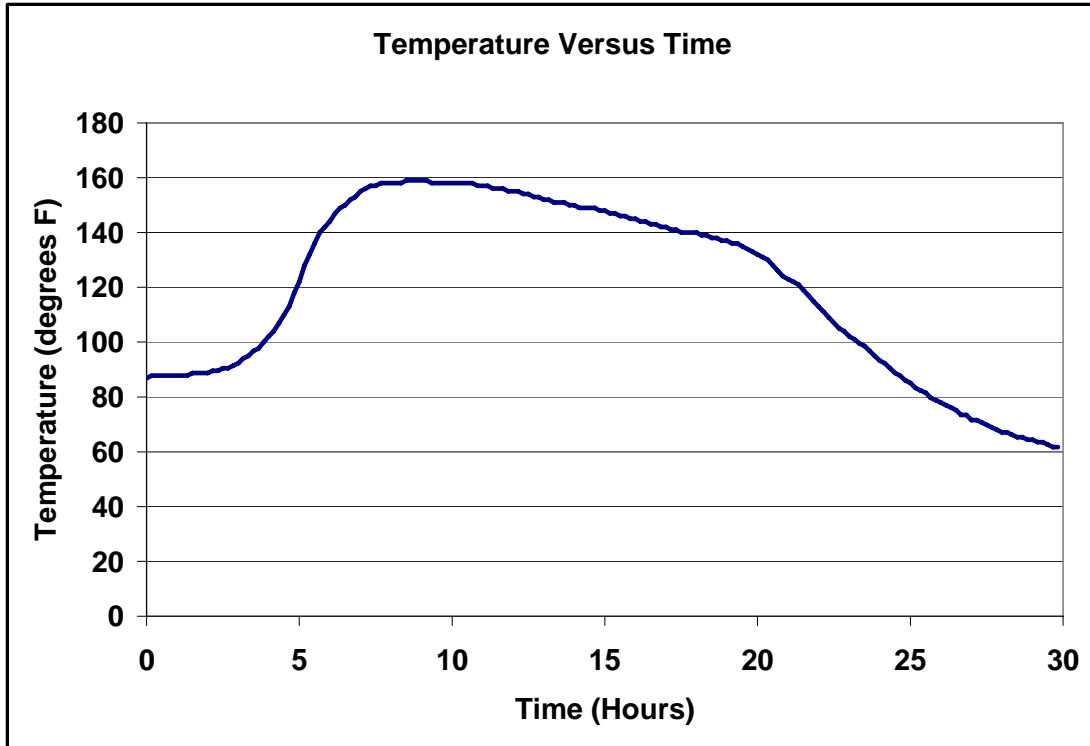


Figure 7.2: Temperature curve during curing for TSB specimen

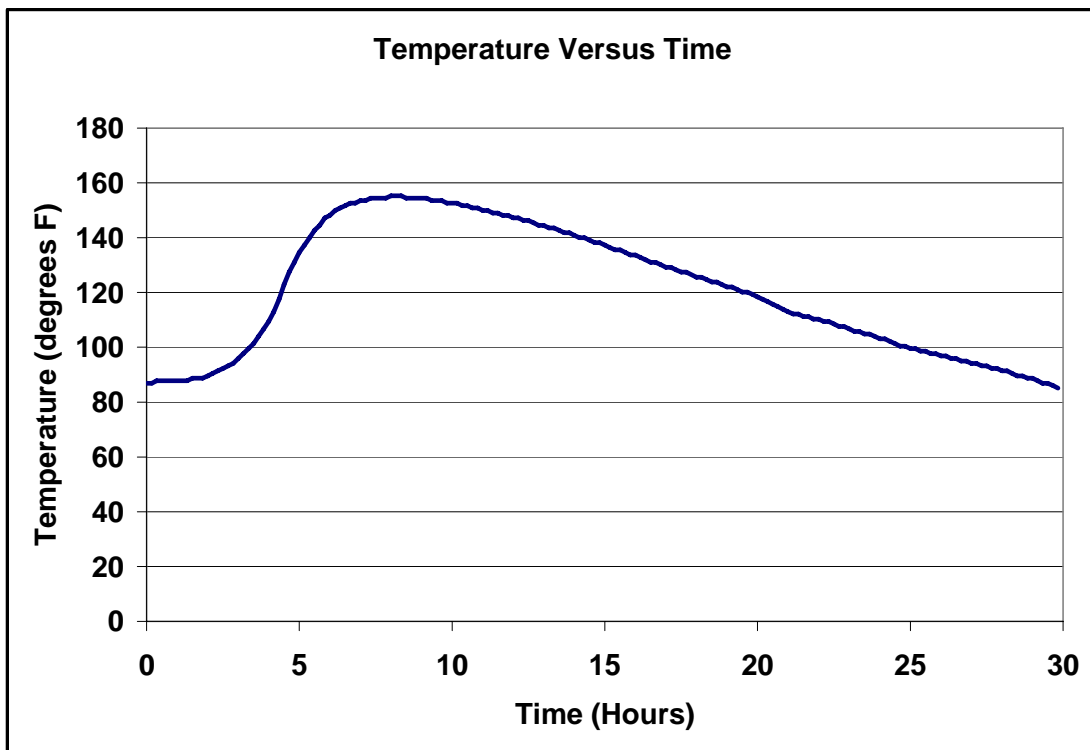


Figure 7.3: Temperature curve during curing for TB specimen

7.2 Transfer Length

As described previously, end-slip measurements were used to evaluate the transfer length of each girder. In these calculations, f_{si} was assumed to be 196 ksi for all single-strand specimens and 192 ksi for the T-beams (loss calculations in A.6).

For all SSB specimens, no end had a longer implied (18-day) transfer length than the value assumed by the AASHTO and ACI codes (33 inches as calculated from equation 1.1). The average 18-day transfer length for the SSB specimens was 21 inches and values for each specimen end can be seen in Table 7.2. However, ACI 11.4.3 for shear design of prestressed members assumes the transfer length to be 50-strand diameters. Although five specimen ends did exceed this limit, the average value was well below the value of 50-strand diameters (25 inches). AASHTO 5.11.4.1 assumes a value of 60-strand diameters (30 inches) for shear design of prestressed members. Only one specimen end exceeded this value. A 15% increase was seen in the transfer length from release to 18 days. From 18 days to testing day, a noticeable increase in transfer length was not seen.

Table 7.2: Implied transfer lengths (in inches) for SSB specimens

Transfer Lengths for <u>Single-Strand Beams</u>								
Beam	Embedment Length	Spread (in)	Release		18 Days		Test Day	
			A	B	A	B	A	B
SSB A	6'-1"	21	16	17	26	30	27	30
SSB B	6'-1"	21	18	24	16	30	16	30
SSB C	6'-1"	21	17	7	24	11	23	11
SSB D	4-10"	22	30	25	29	31	29	31
SSB E	4-10"	22	19	19	13	17	14	17
SSB F	4-10"	22	12	15	10	16	10	16
Average			18		21		21	

The average 18-day implied transfer length for the TSB specimens was 28 inches, once again below the implied transfer length value predicted by the AASHTO and ACI code provisions. Values for each specimen end can be seen in Table 7.3. There were several specimen ends that did exceed the 25-inch (ACI) and 30-inch (AASHTO) assumed values that ACI and AASHTO require for shear design. Unlike the SSB specimens, a noticeable increase in transfer length was seen from release to 18 days. This value was close to 100%. Just like the SSB specimens, a noticeable increase from 18 days to testing day was not seen.

Table 7.3: Implied transfer lengths (in inches) for TSB specimens

Transfer Lengths for <u>T</u>op-<u>S</u>trand <u>B</u>eams								
Beam	Embedment Length	Spread (in)	Release		18 Days		Test Day	
			A	B	A	B	A	B
TSB A	4'-10"	28	17	19	30	34	30	34
TSB B	4'-10"	28	21	13	30	24	30	25
TSB C	4'-10"	28	15	13	34	31	34	31
TSB D	6'-1"	28	15	17	22	19	23	19
TSB E	6'-1"	28	8	21	20	31	22	31
TSB F	6'-1"	28	8	15	32	23	36	25
Average			15		28		28	

The average 18-day implied transfer length for the TB specimens was 26 inches, once again below the implied transfer length (32 inches) value predicted by the AASHTO and ACI code provisions. Values for each specimen end can be seen in Table 7.4. There were several specimen ends that did exceed the 25-inch (ACI) and

30-inch (AASHTO) assumed values that ACI and AASHTO require for shear design. Similar to the SSB specimens, a noticeable increase in transfer length was not seen from release to 18 days and from 18 days to testing.

Table 7.4: Implied transfer lengths (in inches) for TB specimens

Transfer Lengths for T-Beams															
Beam-Side	Release					18 Days					Test Day				
	A	B	C	D	E	A	B	C	D	E	A	B	C	D	E
A1			19	25	6			28	34	13			28	34	14
A2	18	28	16	41	20	24	36	30	44	25	25	36	30	44	25
B1		11	40	19	7		22	41	11	16		22	41	15	17
B2	11				6	14				8	18				11
C1	20	18	25	28	19	23	20	28	31	17	23	20	28	31	19
C2	26	28	42	31	25	28	38	42	40	31	28	38	42	41	31
D1	28	32		11	10	30	35		15	21	30	35		16	22
D2	22	28	17	30	20	25	22	19	31	21	25	24	20	31	22
Ave	22					26					27				

Increases in transfer length over time for the specimens with strands less than 12 inches above the bottom were in general accordance with results by Barnes et al. Barnes et al. found that the transfer lengths were found to increase approximately 10 to 20% over time, on average. All specimens that had the strand cast only two inches above the bottom (SSB and T-beam specimens) were found to increase approximately 10 to 20%. The TSB specimens had an increased implied transfer length of nearly 100% and this could be attributed to the “top-strand” effect. Russell and Burns also completed a study on transfer lengths and found similar results.

Zia and Mostafa, Cousins et al., Mitchell et al., Buckner, Russell and Burns and Barnes et al. all proposed equations for estimating transfer lengths. These equations are given in Chapter Two of this manuscript. The equation given by Buckner is the current transfer length implied by the ACI code. The experimental results are compared

against other equations and are graphed in Figure 7.4. The vertical line represents the range of the experimental results.

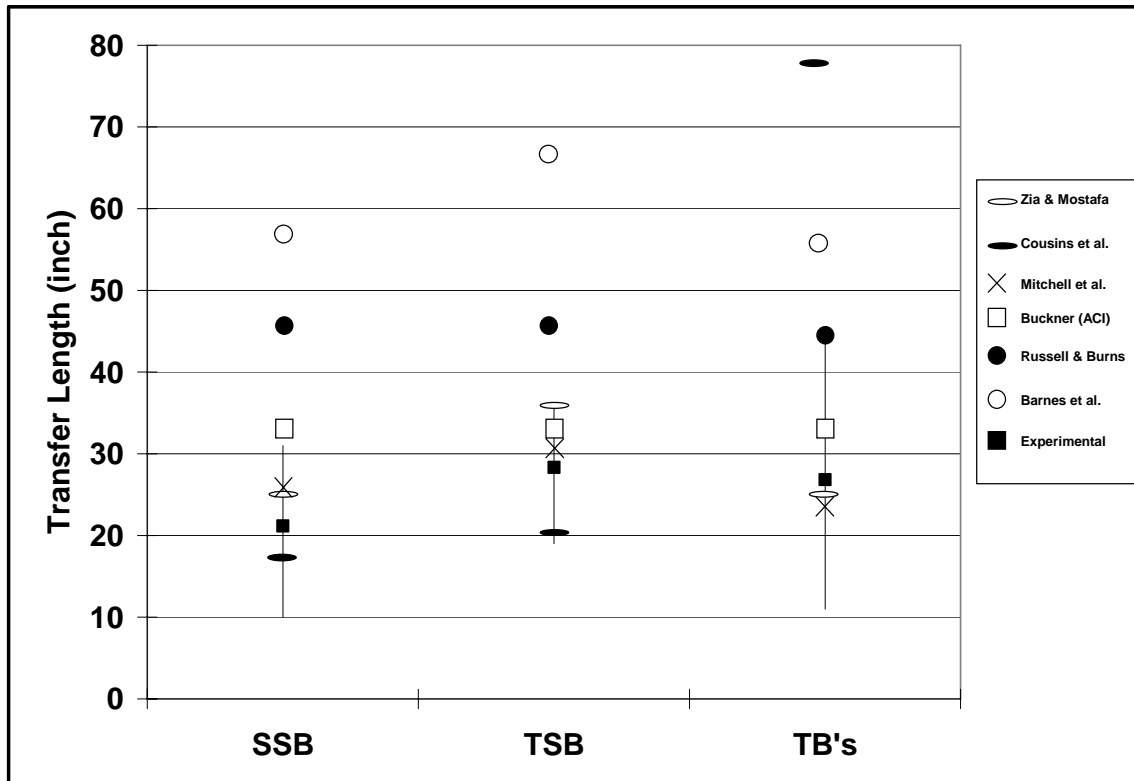


Figure 7.4: Experimental results for transfer length versus other prediction models

7.3 Development Length

Flexural failure by strand rupture was the failure mode of all specimens tested. In each case, the failure moment exceeded the calculated nominal-moment capacities by 10 to 20% for specimens with an embedment length of 6'-1". All specimens with an embedment length of 4'-10" had an increase of 25 to 35% over the calculated partially-developed nominal capacity. It must be noted that a decreased nominal-moment capacity was calculated for specimens with an embedment length shorter than the calculated development length. Calculations for both the fully-developed and partially-developed nominal moment capacities can be found in sections A.4 and A.5. Table 7.5

presents all results of the specimens tested. Furthermore, the maximum end slip recorded for all specimens during testing was less than 0.01 inches.

Table 7.5: Summary of tested specimens

	Beam	% I_e	Nominal Moment (M_n)	Experimental Moment (M_{exp})	M_{exp}/M_n	Strand Rupture	Strand Slip >0.01 in.
Bottom Strand	SSB A	100	33.0	36.6	1.11	Yes	No
	SSB C	100	33.0	38.2	1.16	Yes	No
	SSB D	80	29.4	39.6	1.35	Yes	No
	SSB E	80	29.4	37.5	1.28	Yes	No
	SSB F	80	29.4	38.8	1.32	Yes	No
Top Strand	TSB A	80	29.4	38.9	1.32	Yes	No
	TSB B	80	29.4	39.1	1.33	Yes	No
	TSB C	80	29.4	38.6	1.31	Yes	No
	TSB D	100	33.0	36.6	1.11	Yes	No
	TSB E	100	33.0	37.3	1.13	Yes	No
	TSB F	100	33.0	35.7	1.08	Yes	No
T-Beams	TB A	100	319	370	1.16	Yes	No
	TB B	100	319	383	1.20	Yes	No
	TB C	80	280	359	1.28	Yes	No
	TB D	80	280	376	1.34	Yes	No

7.3.1 SSB Specimen Flexural Results

A moment versus deflection graph for each SSB specimen shows that each one surpassed its nominal-moment capacity and that each failure by strand rupture, Figures 7.5 – 7.14. Also, end slip during loading is plotted for each specimen.

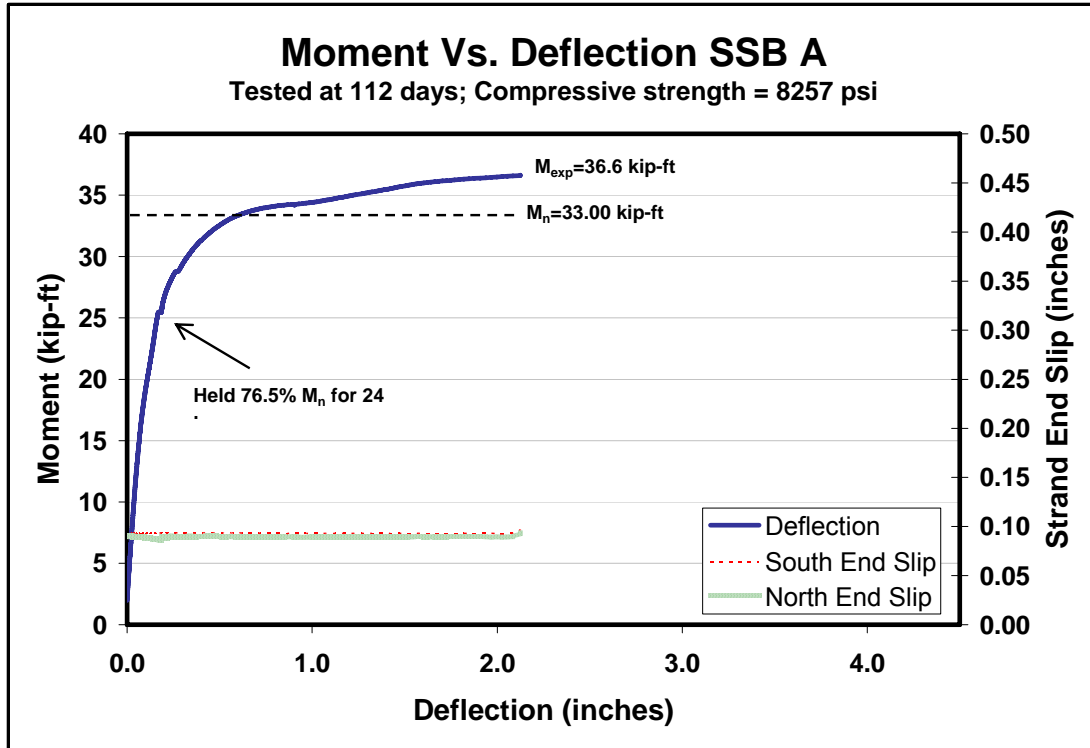


Figure 7.5: Moment versus deflection for SSB A



Figure 7.6: Failure of SSB A

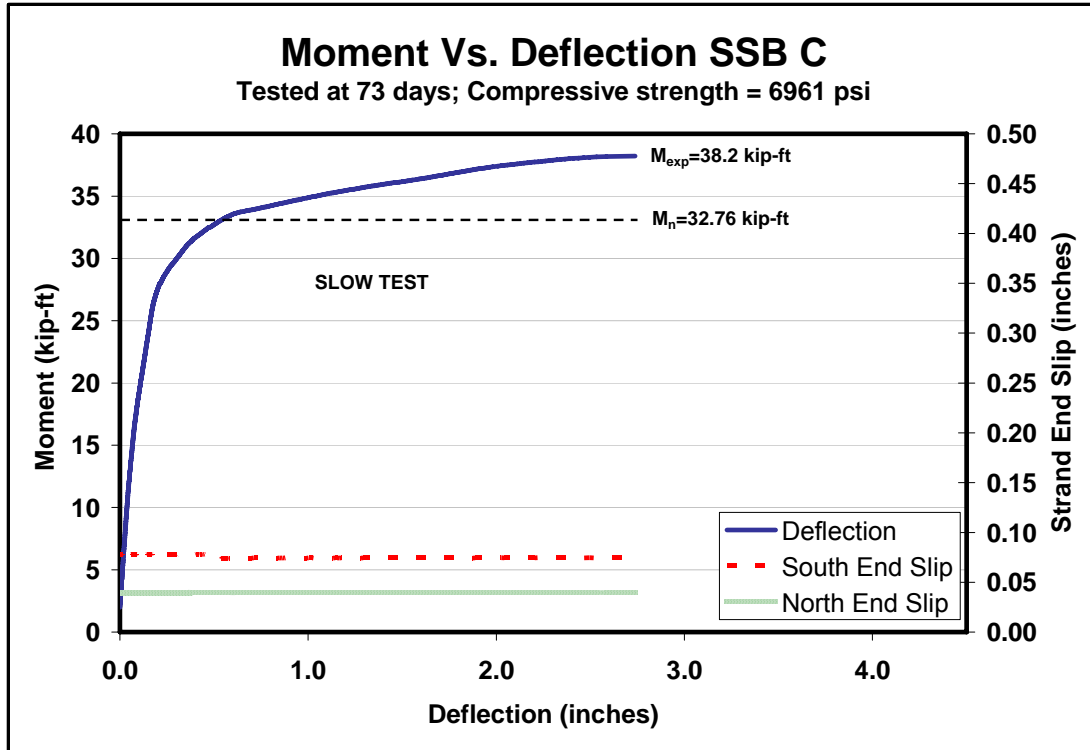


Figure 7.7: Moment versus deflection for SSB C



Figure 7.8: Failure of SSB C

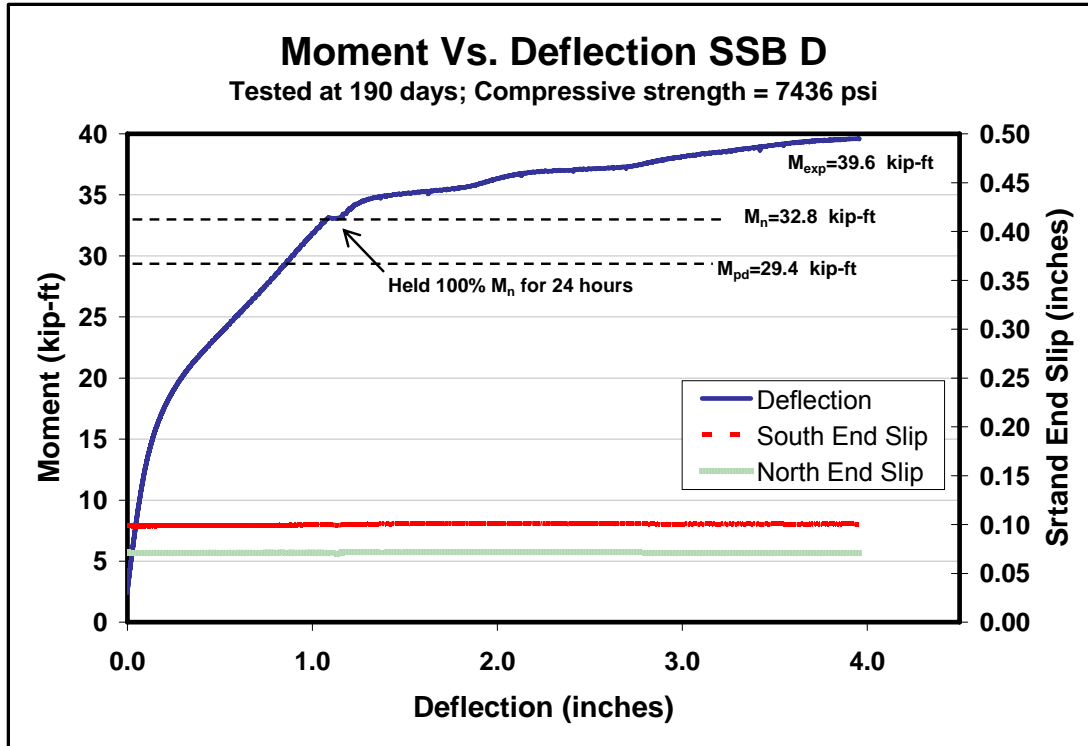


Figure 7.9: Moment versus deflection for SSB D



Figure 7.10: Failure of SSB D

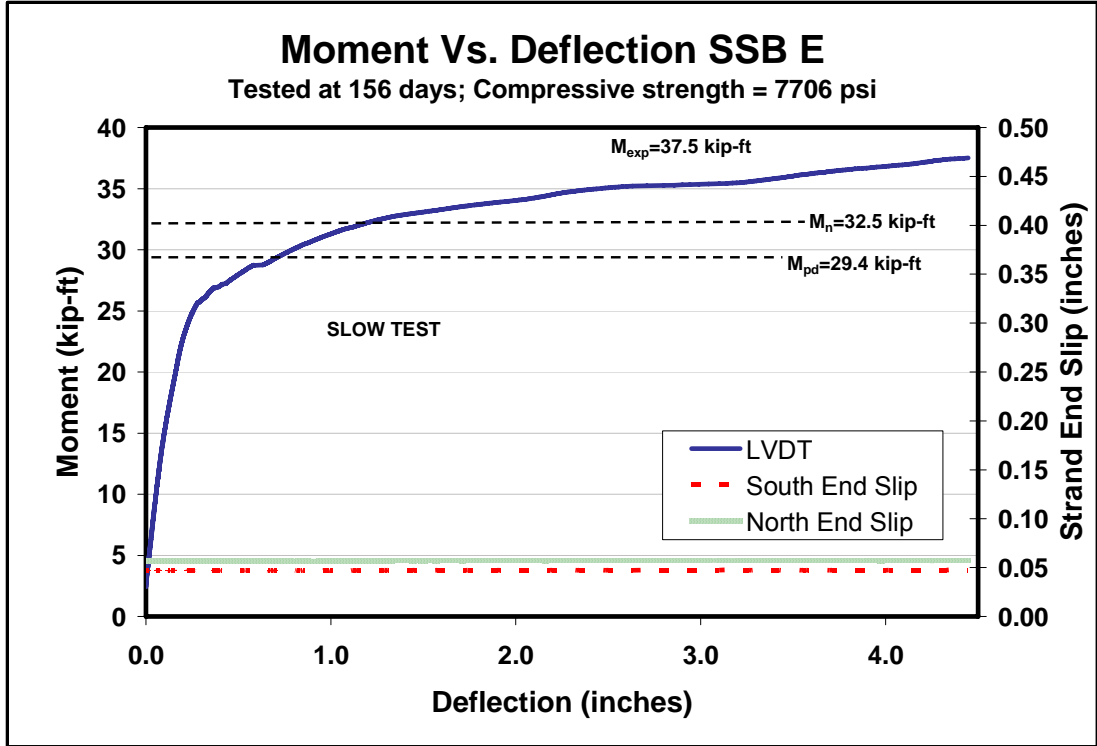


Figure 7.11: Moment versus deflection for SSB E



Figure 7.12: Failure of SSB E

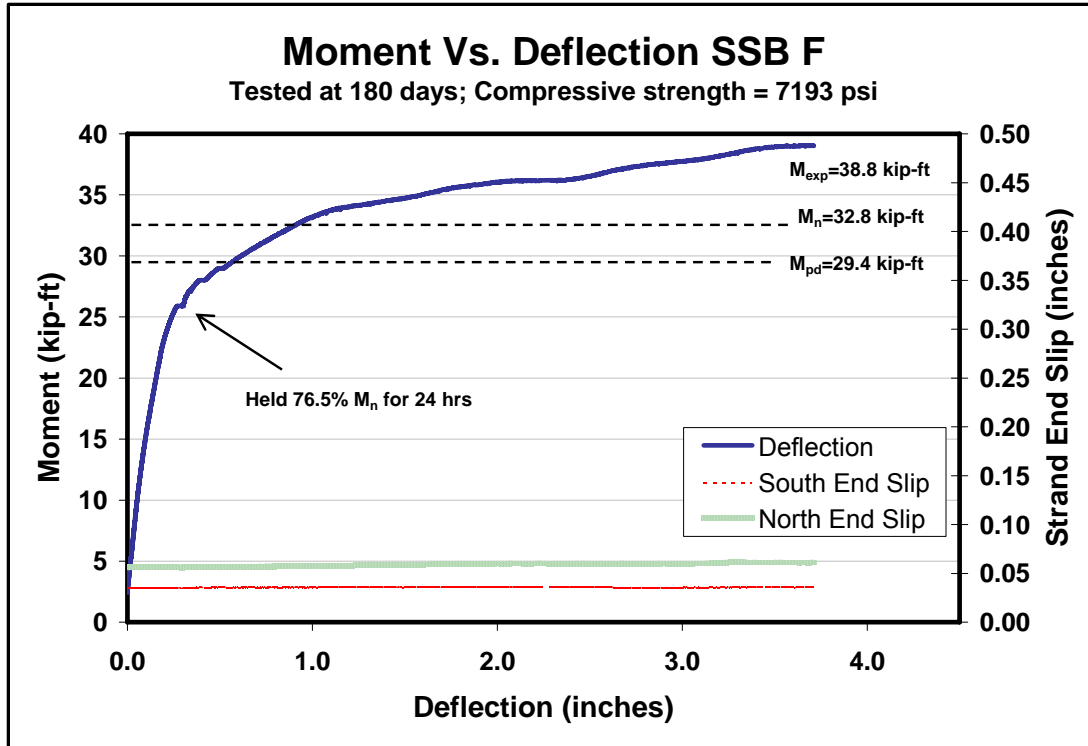


Figure 7.13: Moment versus deflection for SSB F



Figure 7.14: Failure of SSB F

7.3.2 TSB Specimen Flexural Results

A moment versus deflection graph for each TSB specimen shows that each one surpassed its nominal-moment capacity and failure by strand rupture, Figures 7.15 – 7.26. Also, end slip during loading is plotted for each specimen.

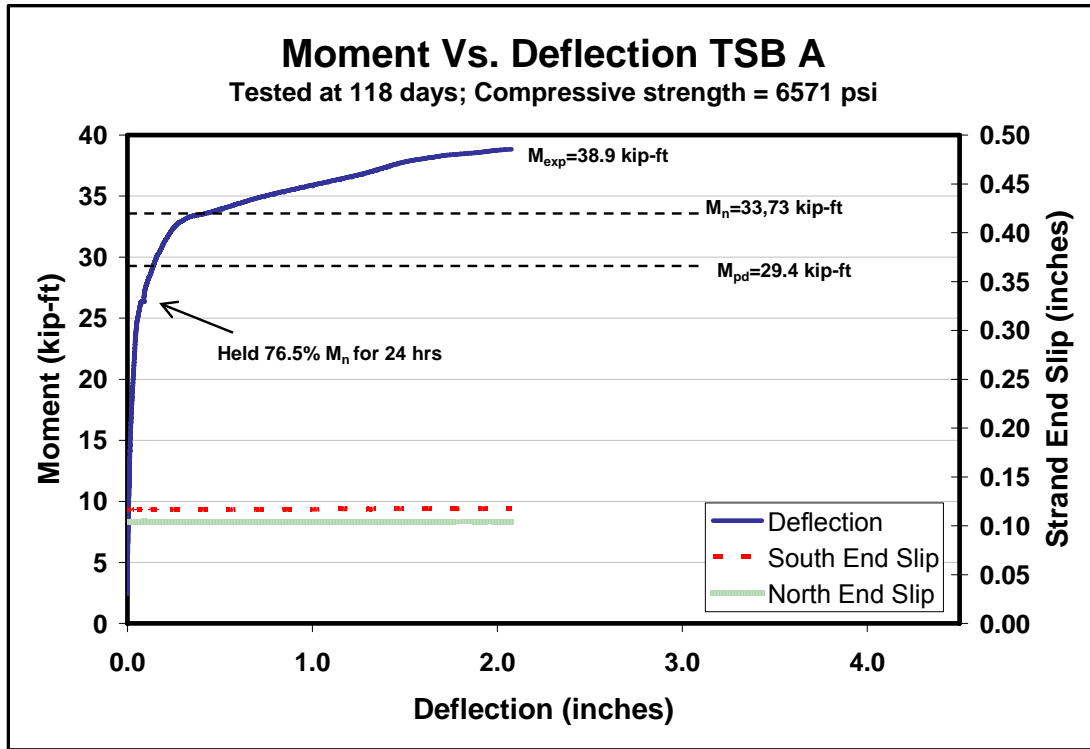


Figure 7.15: Moment versus deflection for TSB A

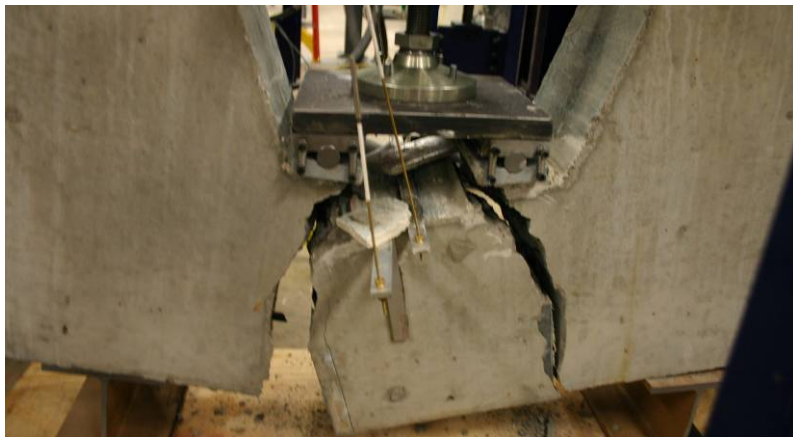


Figure 7.16: Failure of TSB A

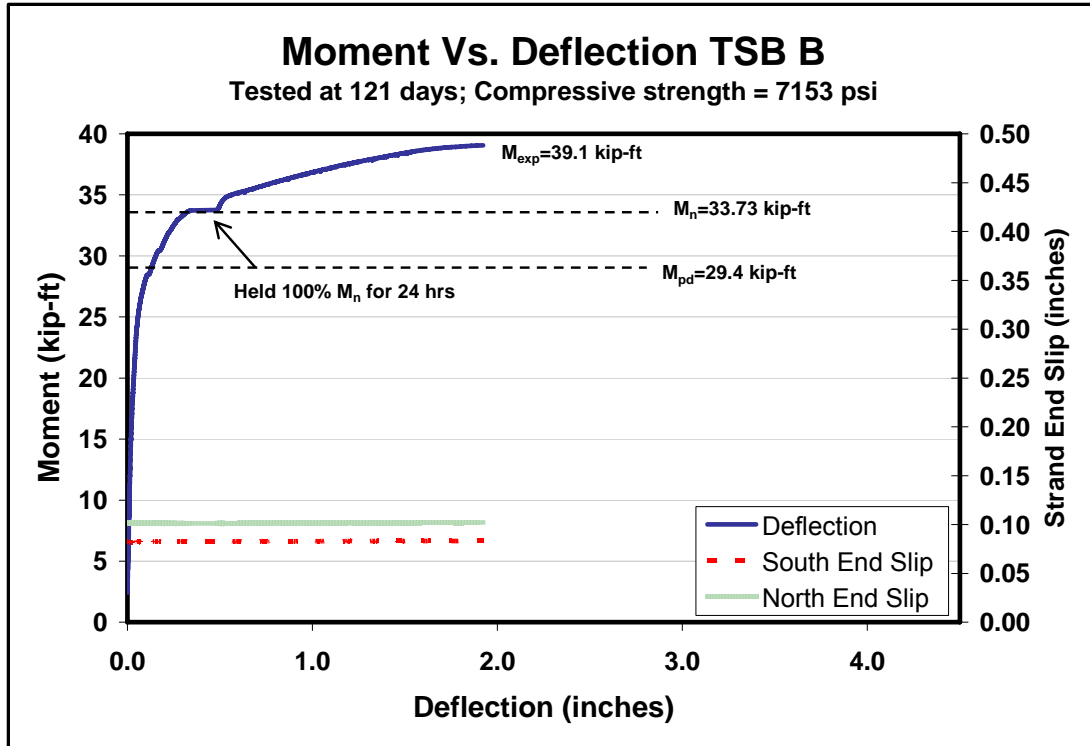


Figure 7.17: Moment versus deflection for TSB B



Figure 7.18: Failure of TSB B

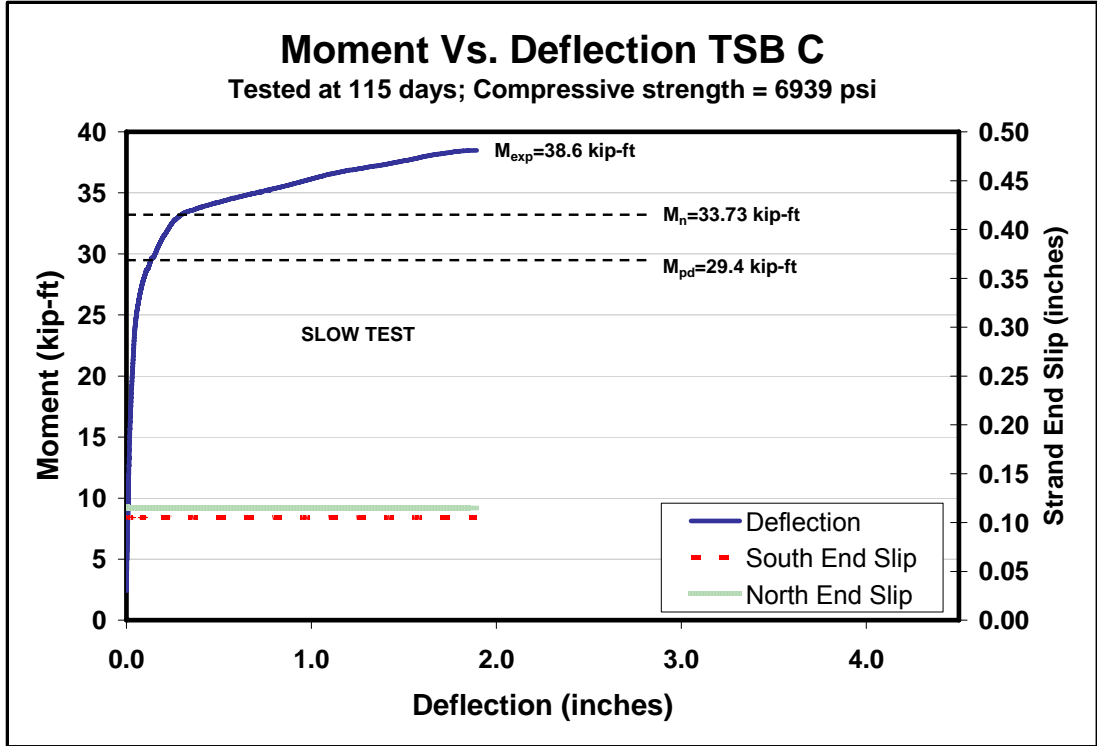


Figure 7.19: Moment versus deflection for TSB C



Figure 7.20: Failure of TSB C

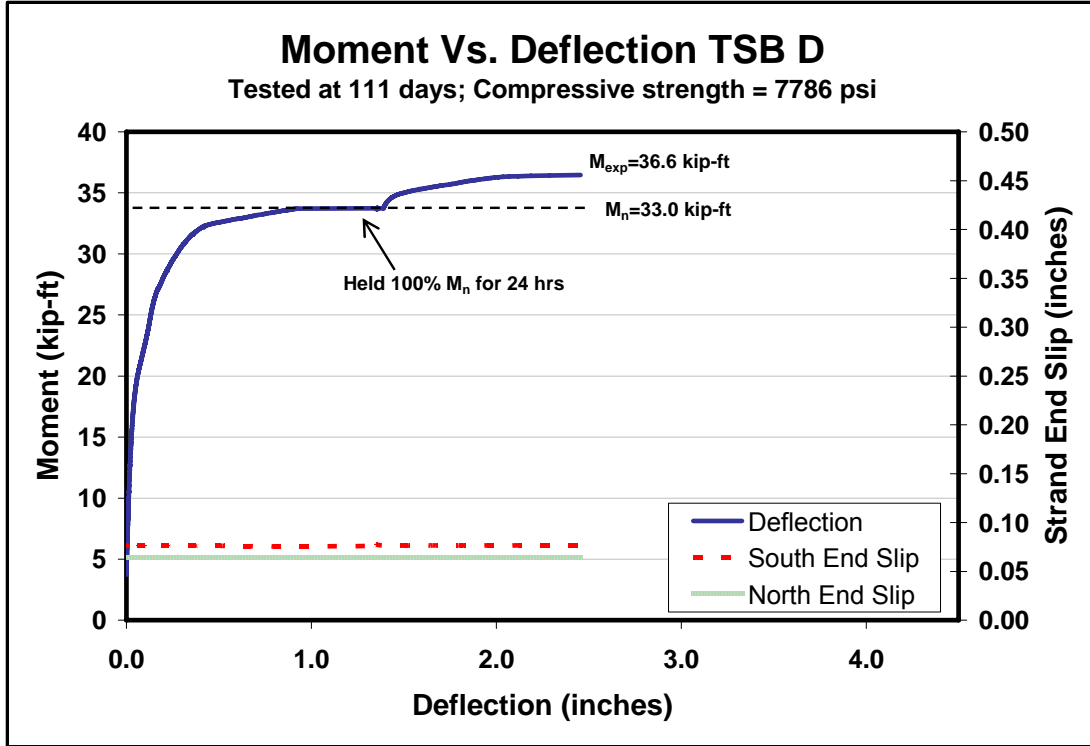


Figure 7.21: Moment versus deflection for TSB D



Figure 7.22: Failure of TSB D

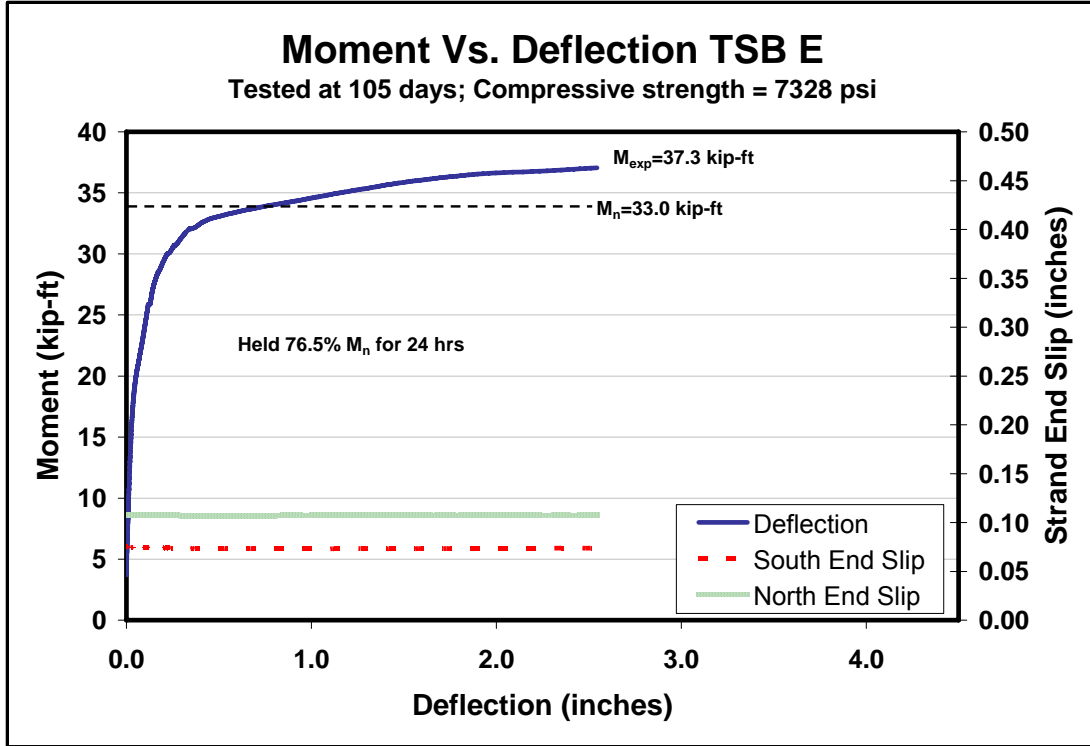


Figure 7.23: Moment versus deflection for TSB E



Figure 7.24: Failure of TSB E

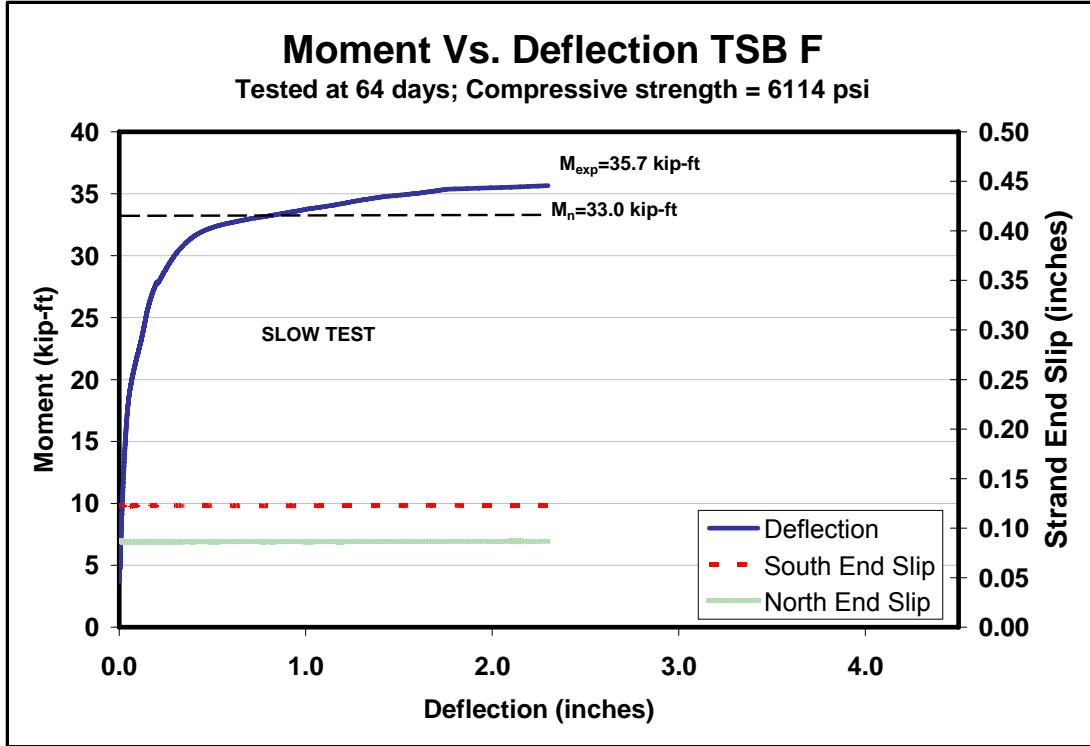


Figure 7.25: Moment versus deflection for TSB F



Figure 7.26: Failure of TSB F

7.3.3 TB Specimen Flexural Results

A moment versus deflection graph for each TB specimen shows that each one surpassed its nominal-moment capacity and failure by strand rupture, Figures 7.27 – 7.34. Also, end slip during loading is not shown as it was for the single-strand specimens because no additional end-slip occurred during the load test to failure.

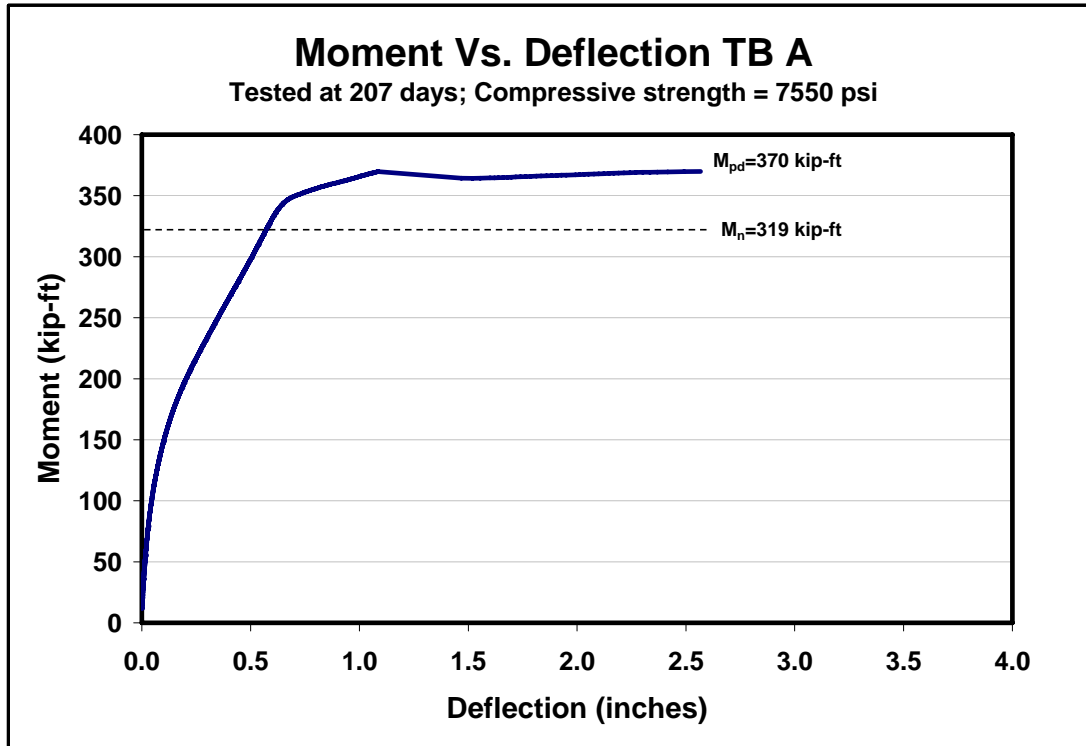


Figure 7.27: Moment versus deflection for specimen TB A



Figure 7.28: Failure of TB A

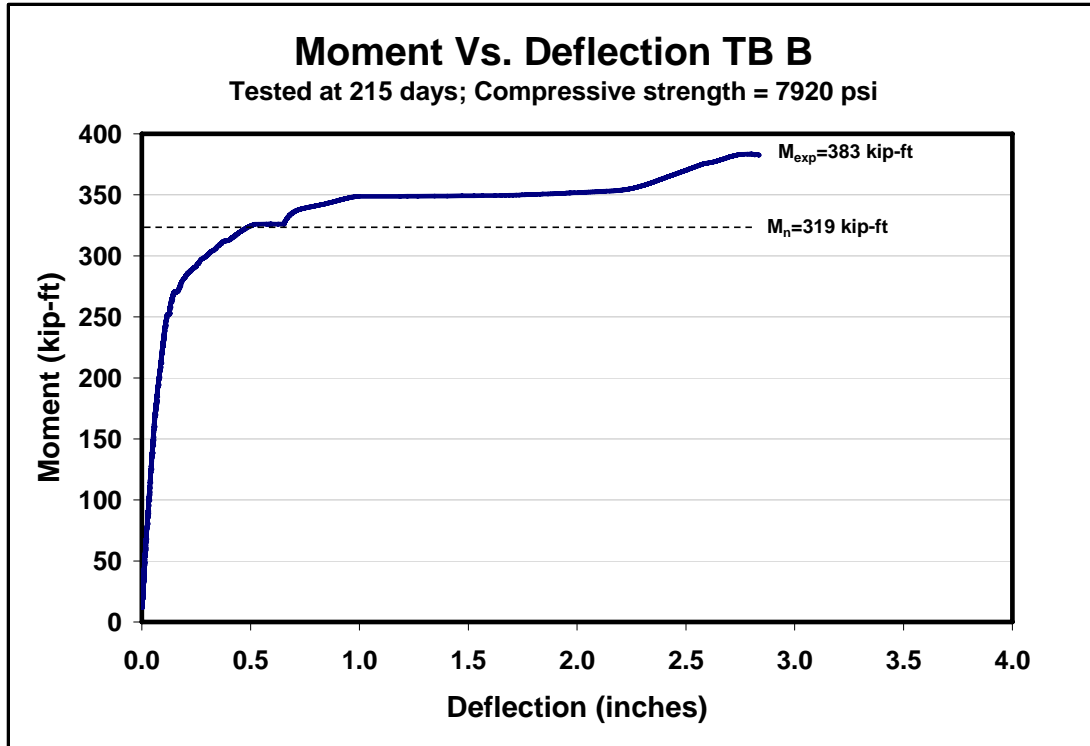


Figure 7.29: Moment versus deflection for specimen TB B

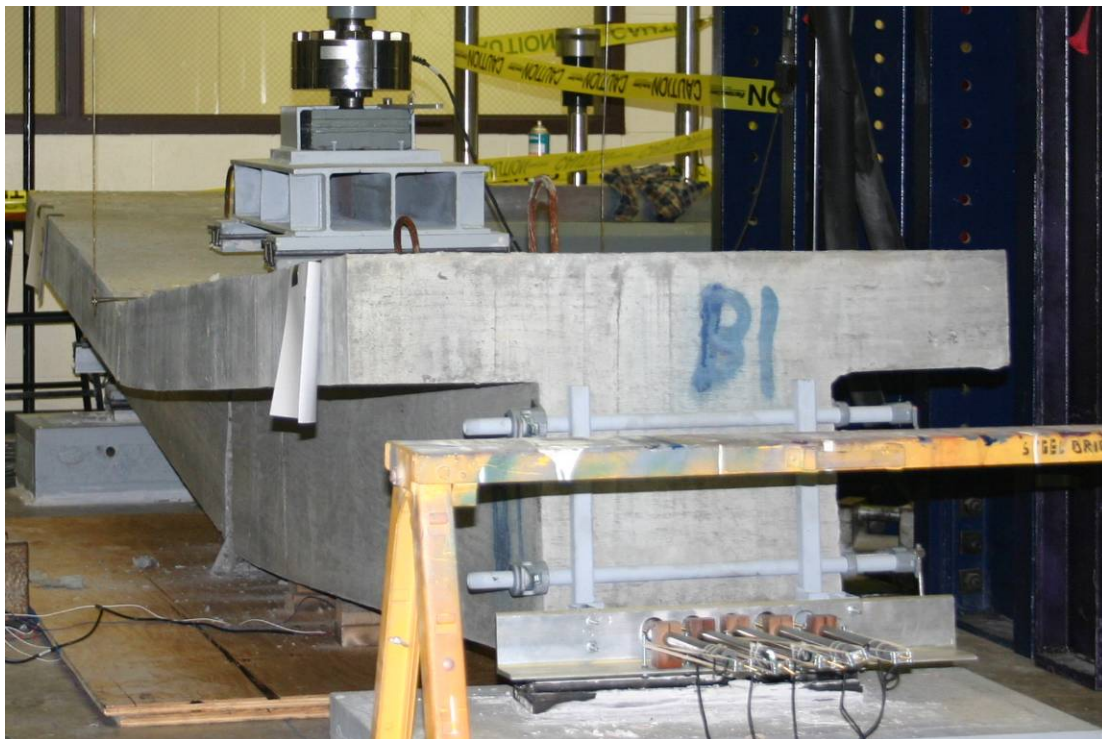


Figure 7.30: Failure of TB B

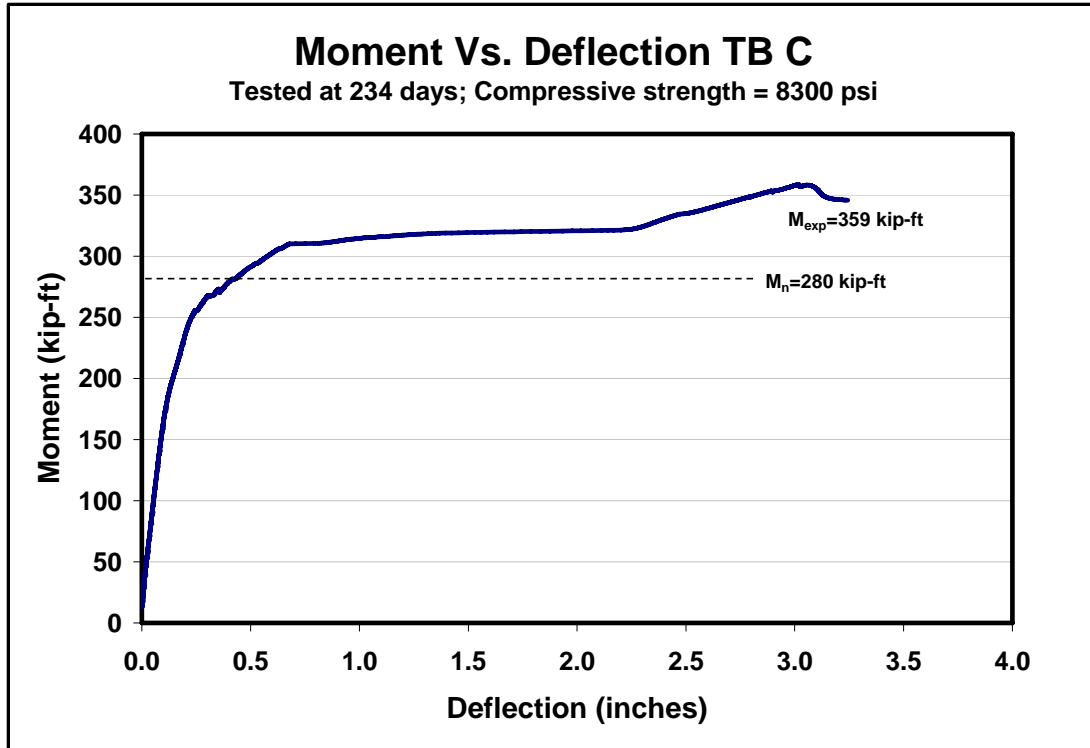


Figure 7.31: Moment versus deflection for specimen TB C



Figure 7.32: Failure of TB C

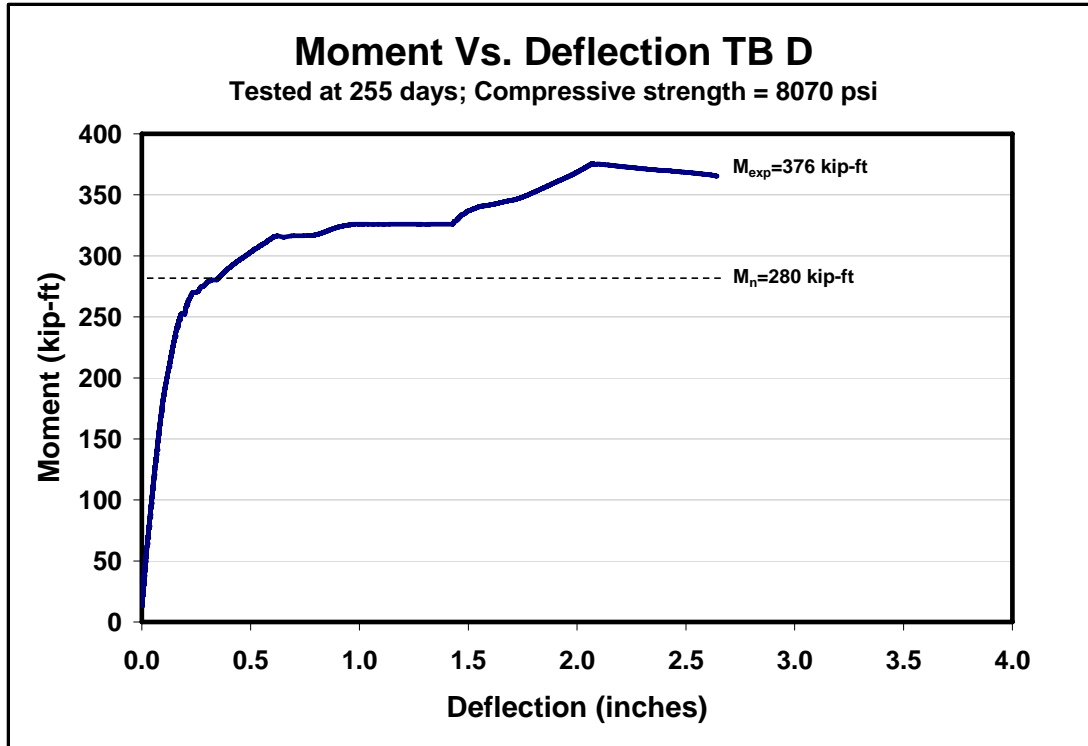


Figure 7.33: Moment versus deflection for specimen TB D



Figure 7.34: Loading of TB D

7.3.4 Comparison of Flexural Results

Figures 7.35 and 7.36 present the moment versus deflection for the single-strand specimens tested at embedment lengths of 6'-1" and 4'-10", respectively. It can be seen that all specimens performed similar. Moment versus deflection curves for the T-beam specimens are shown in the same graph (Figure 7.37).

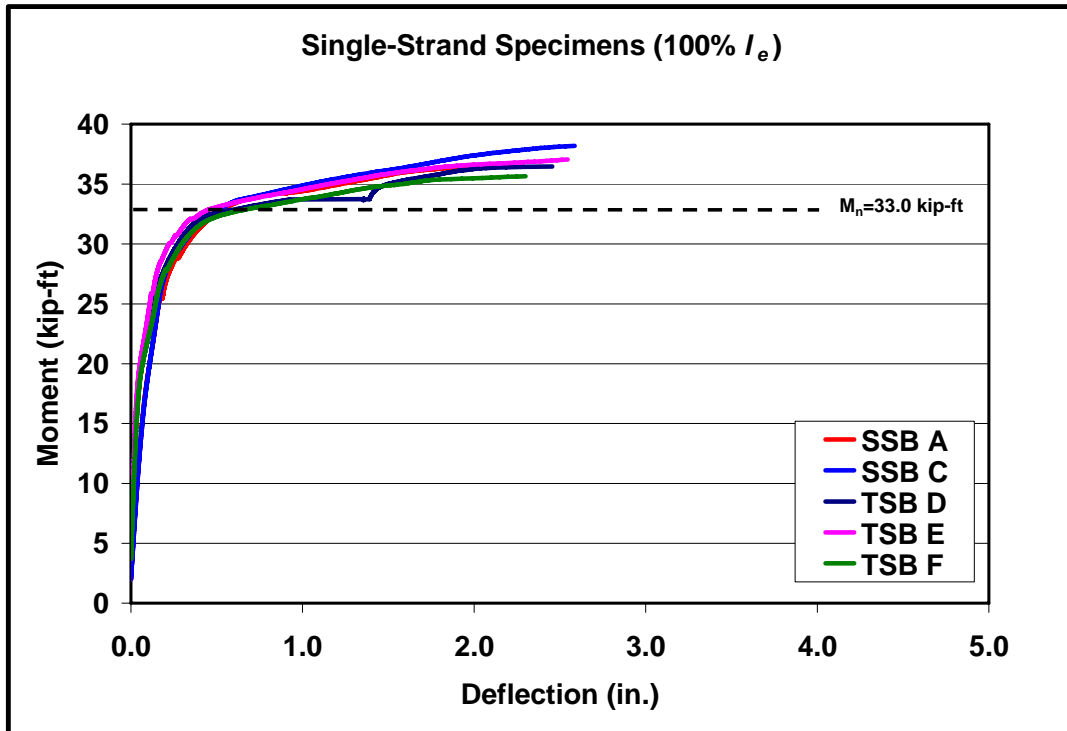


Figure 7.35: Moment versus deflection for all single strand specimens with 100% I_e

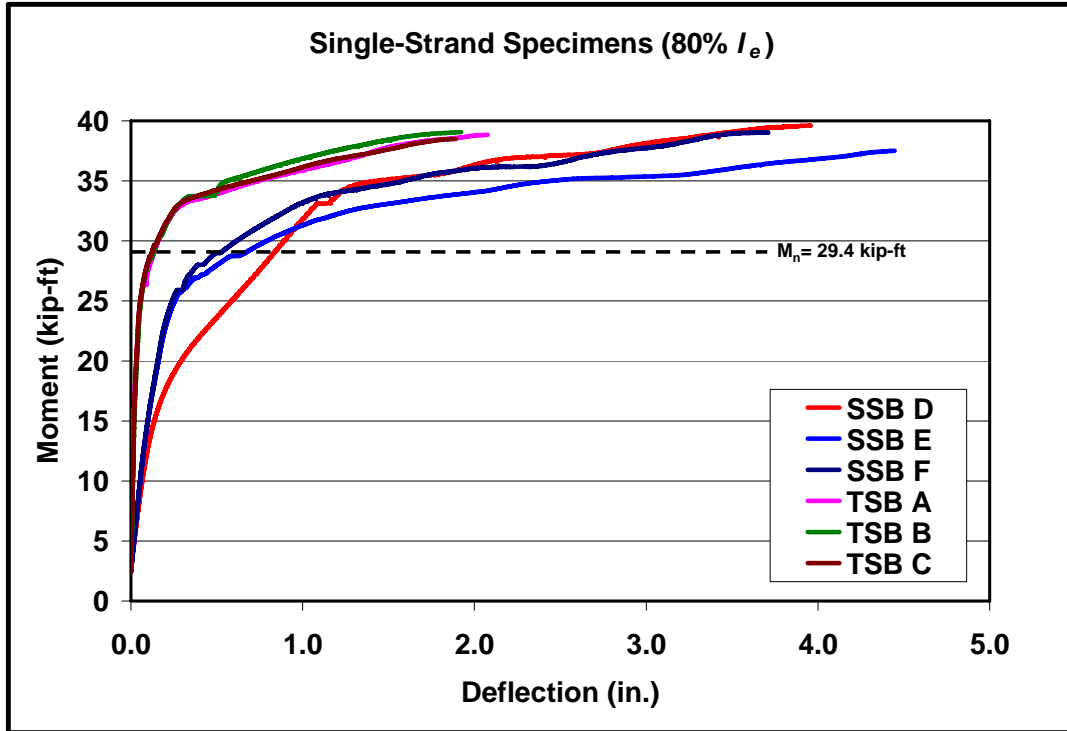


Figure 7.36: Moment versus deflection for all single strand specimens with 80% I_e

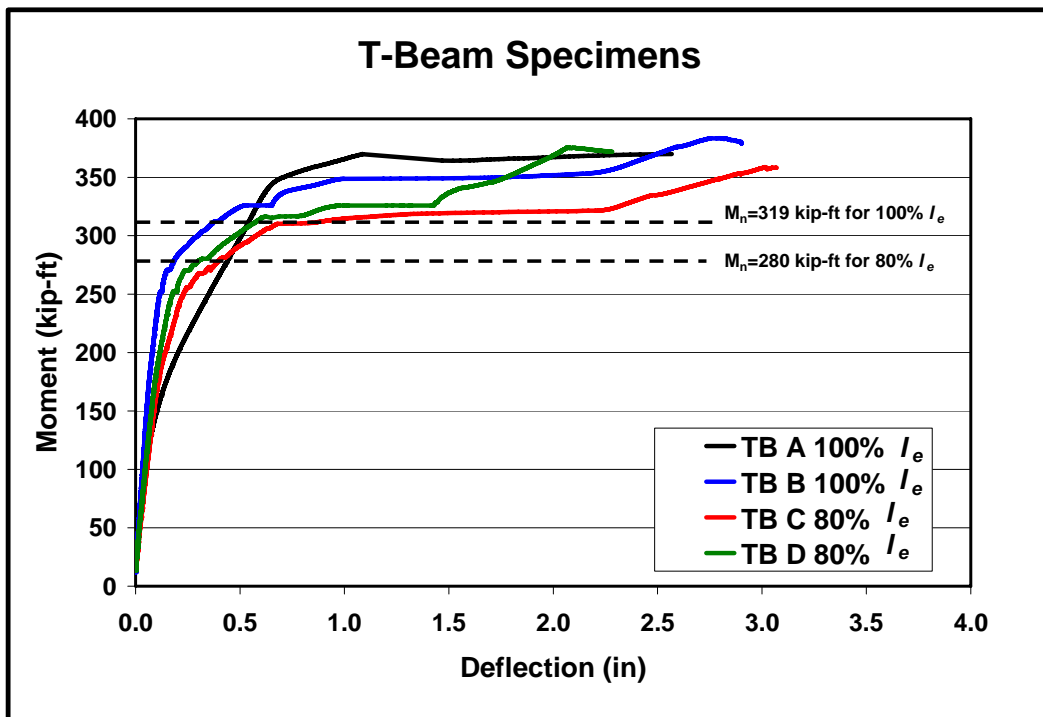


Figure 7.37: Moment versus deflection for all TB specimens

7.4 VWSG Results

As noted in a Chapter Six, VWSGs were embedded in three of the flexural specimens, SSB A, TSB D, and TB A. Gages were used to evaluate time-dependent deformations and compare with those predicted with code expressions. Prestress losses were calculated with the PCI method and the comparisons with experimental results can be shown in Tables 7.6-7.8. On average, the difference between the code predictions and experimental results are between 3-6 ksi.

Table 7.6: Comparison of prestress losses for SSB A

Time (Days)	PCI	Experimental
Release	196	198
2	196	197
8	191	194
17	189	193
23	189	190
35	188	191
55	187	190
84	186	189
111	185	188

Note: all values in ksi

Table 7.7: Comparison of prestress losses for TSB D

Time (Days)	PCI	Experimental
Release	196	199
11	190	197
45	187	194
74	186	193
103	185	191
104	185	191
109	185	191

Note: all values in ksi

Table 7.8: Comparison of prestress losses for TB A

Time (Days)	PCI	Experimental
Release	192	195
2	189	193
8	186	191
17	183	190
23	183	188
35	181	187
55	180	185
84	179	184
205	177	179

Note: all values in ksi

CHAPTER EIGHT - DESIGN AND FABRICATION OF IT SPECIMENS

Inverted-T (IT)-shaped girders were cast in order to determine the long-term prestress losses of prestressed members cast with the proposed SCC mixture. Creep and shrinkage were isolated from one another and time-dependent losses of both these factors were determined.

8.1 IT Properties

Four ITs, twelve feet in length, were cast in order to determine the time-dependent losses of bridge girders with SCC. A twelve-foot length was considered to be adequate for this SCC mixture because previous tests concluded that a six-foot development length was more than adequate to achieve full bond. The girder type used for this part of the project was the IT600. The name is a metric designation and the 600 refers to the girder cross section being 600 mm in width at the bottom and 600 mm in height. The cross section for the IT600 can be seen in Figure 8.1. Table 8.1 presents geometric properties and other useful properties of the IT600. Since the cast specimens differed slightly from the dimensions on the plans, actual dimensions of the specimens were measured and then used for all calculations.

Of the four girders cast, two had the prestressing strand stressed to 75% of the guaranteed ultimate tensile stress (f_{pu}). These two specimens were designated as FT #1 and FT #2, where FT stands for fully tensioned. FT #1 and FT #2 were used to determine the combined long-term effects of creep, shrinkage, and relaxation. Elastic shortening, which is determined just after detensioning, was also determined from these specimens. In addition, the two fully tensioned specimens were used to evaluate transfer lengths by the method discussed in Chapter 5.